

Structural characterization of materials using Powder x-ray diffraction

N. P. Lalla

UGC-DAE Consortium for Scientific Research
Khandwa Road University Campus
Indore.

Contents:

1. Reciprocal Lattice
2. X-ray scattering (Kinematical Approach)
5. Experimental Examples.

Acknowledgements

Dr. B. A. Dassanacharya,

Dr. P.Chaddah,

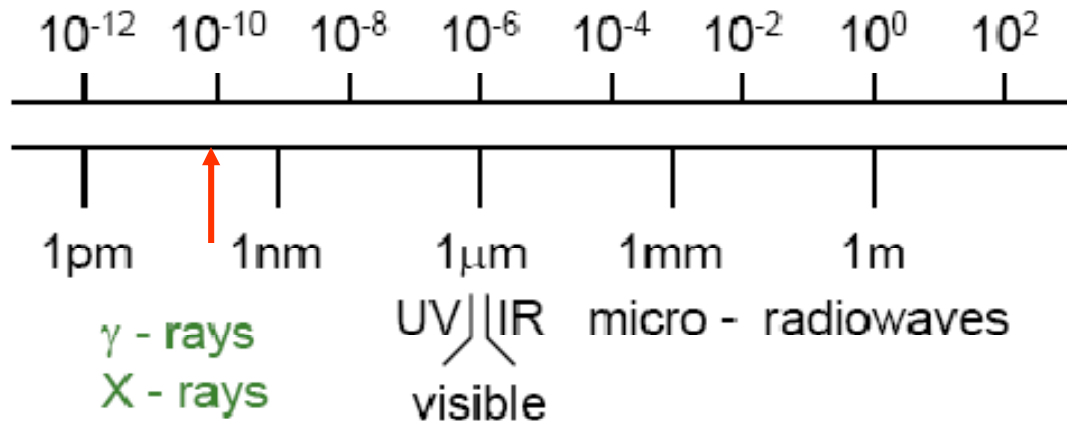
Prof. Ajay Gupta,

Prof. V.N . Bhoraskar,

Prof. O. N. Srivastava,

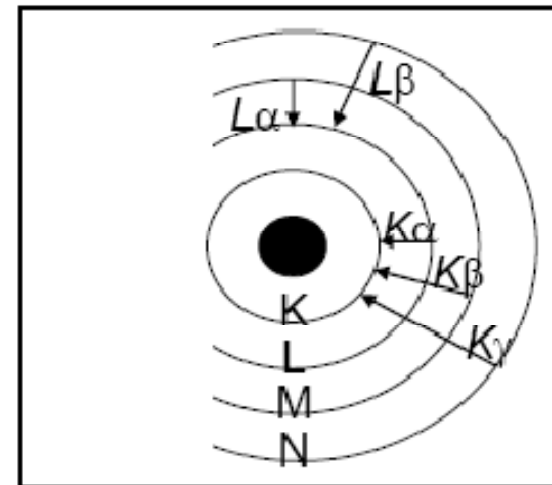
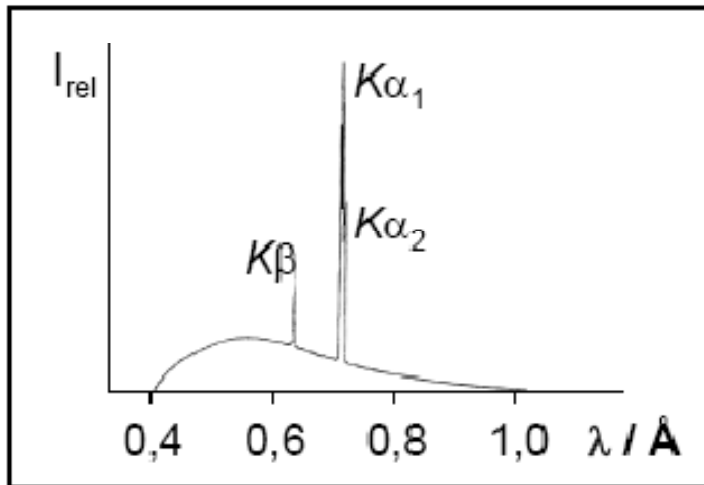
Prof. D. Pandey

X-Rays



$$E = h\nu = \frac{hc}{\lambda}$$

$$\lambda(\text{\AA}) = \frac{12.4}{E(\text{keV})}$$



Discovery of X-rays

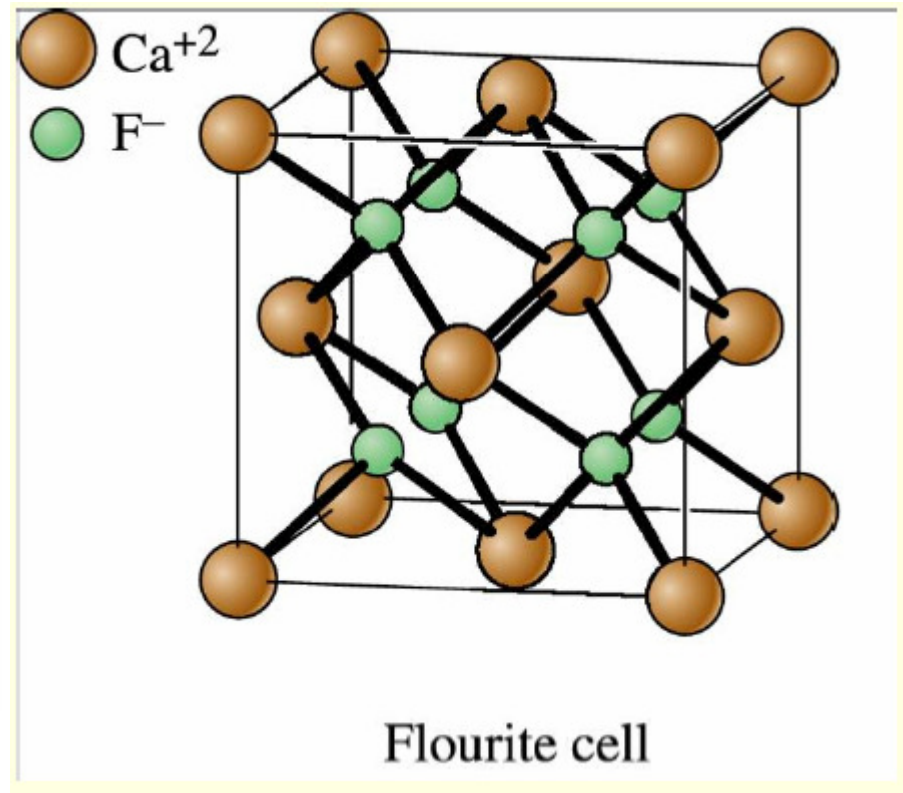
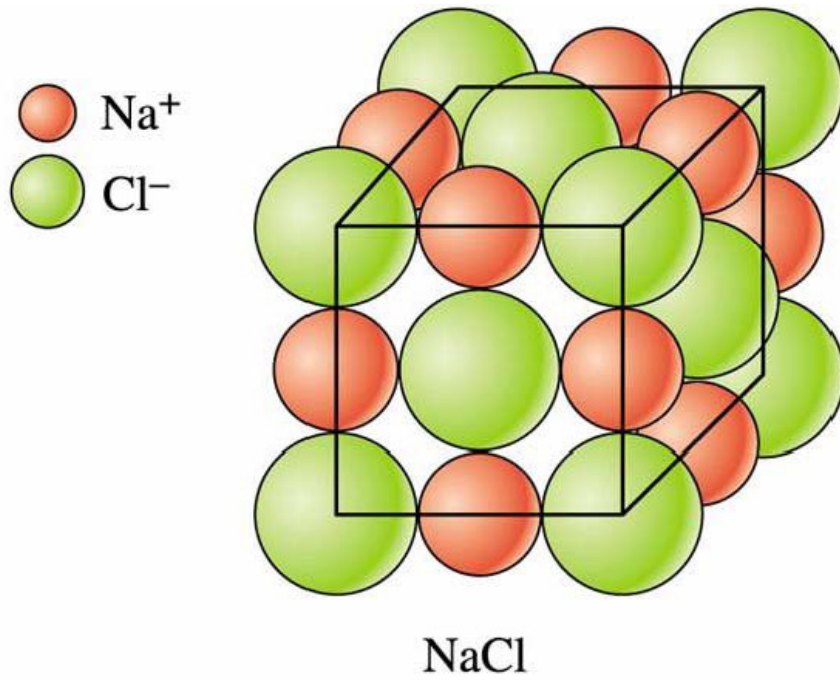


Wilhelm Conrad Röntgen,
our hero

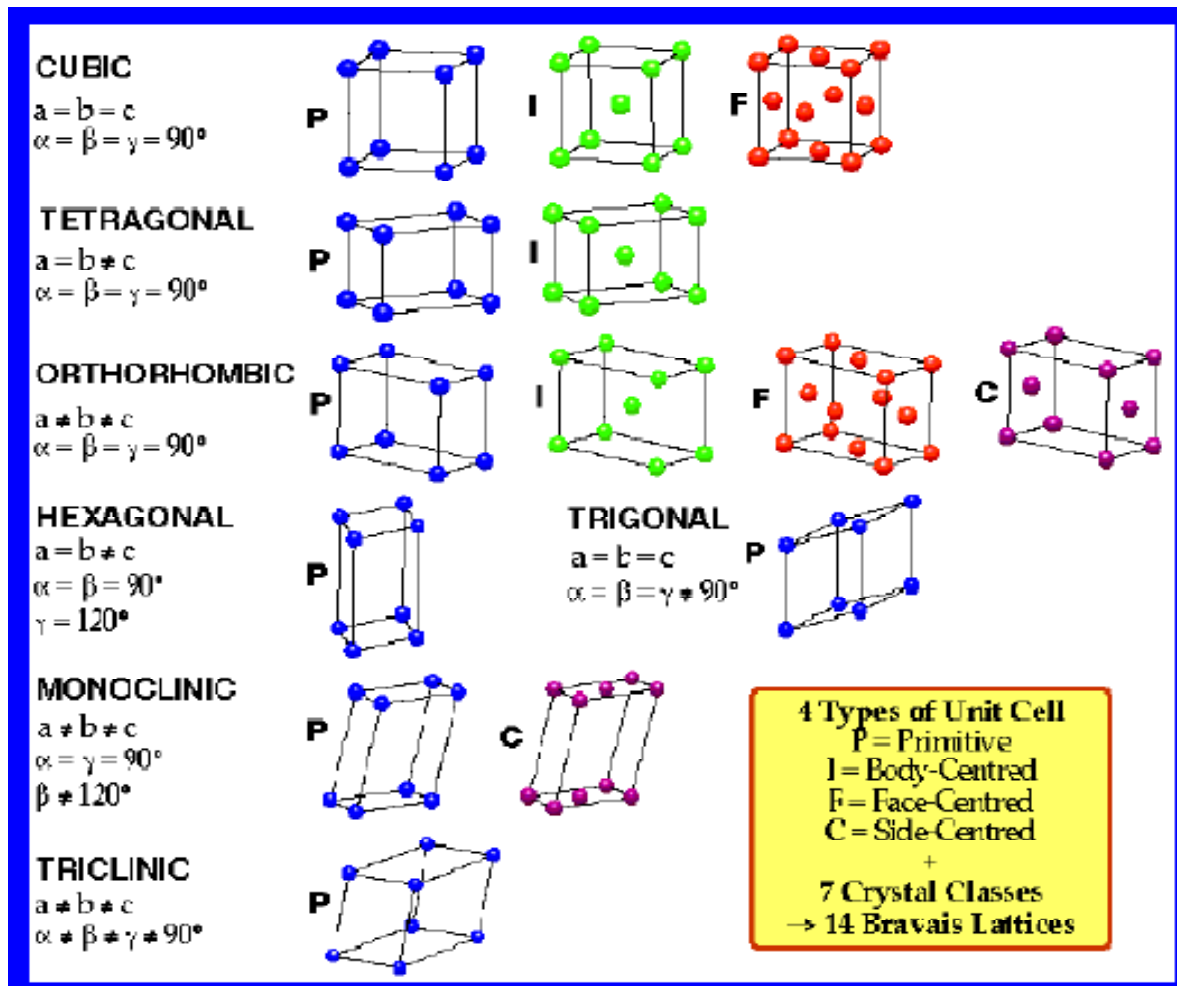


Hand of
Bertha Röntgen
exposure 20 min,
8 Nov 1895

Crystalline materials



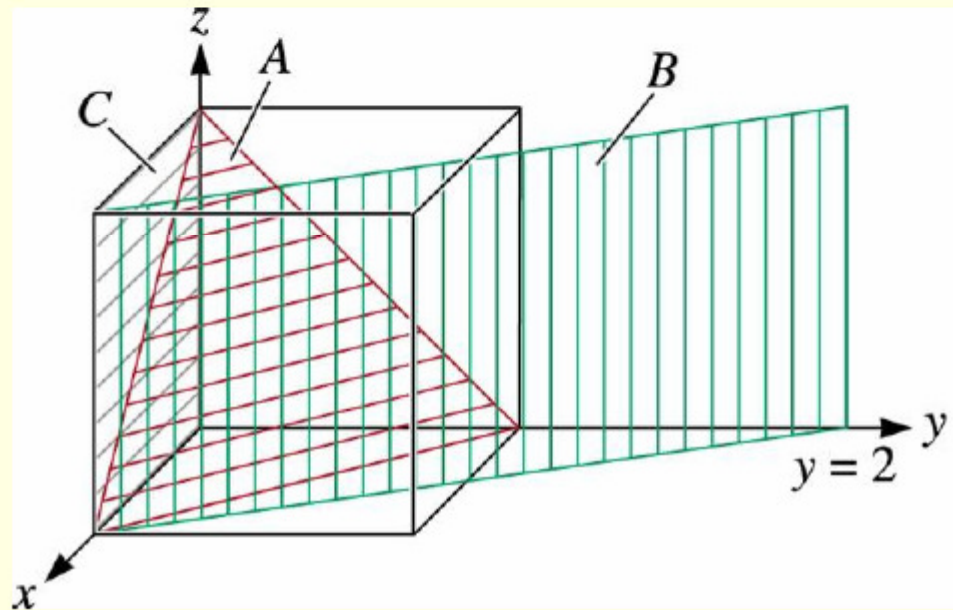
Bravais Lattices



32-Point Groups

230-Space Groups

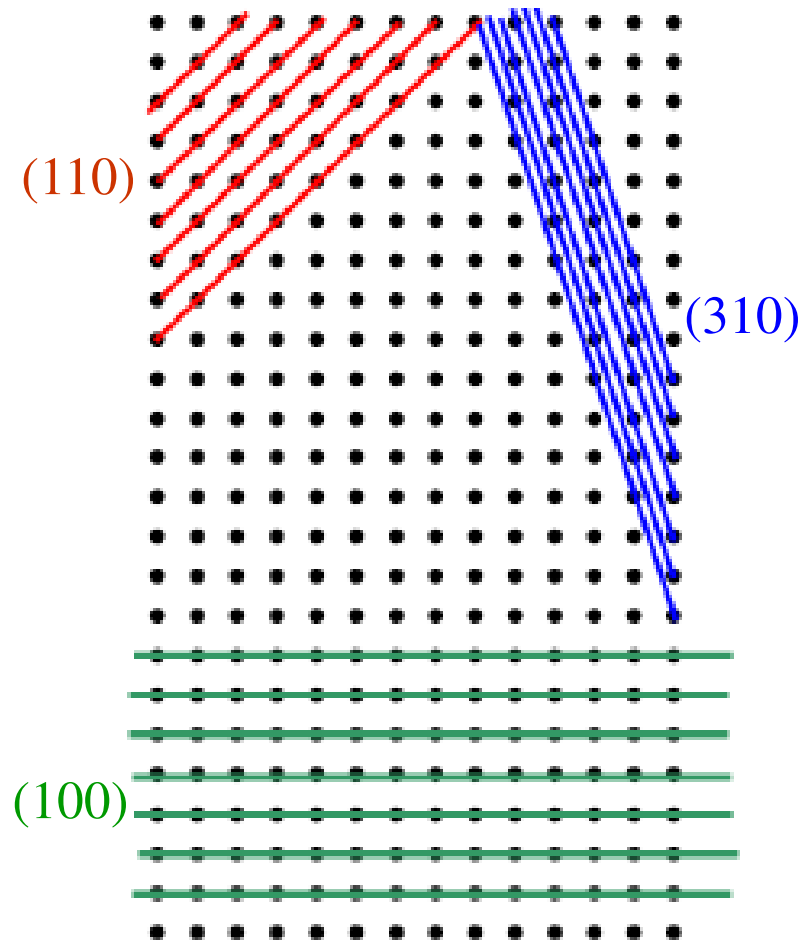
Planes



G. Selvadurai - SJSU - Fall 2006

Crystallographic planes and intercepts

Possible Lattice planes



X-Ray Scattering from periodic Arrangement of Atoms

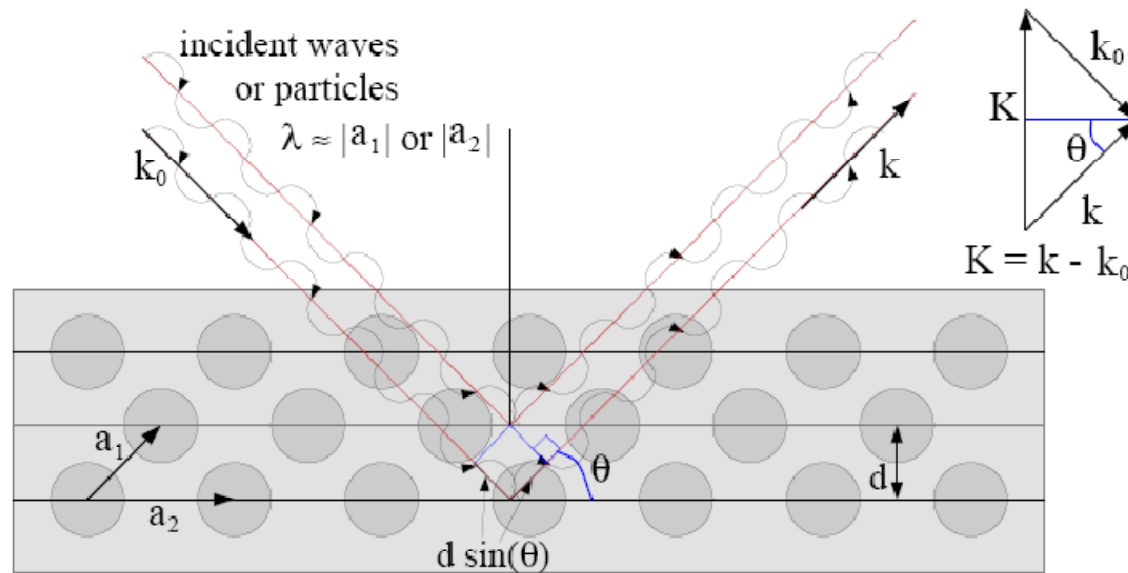
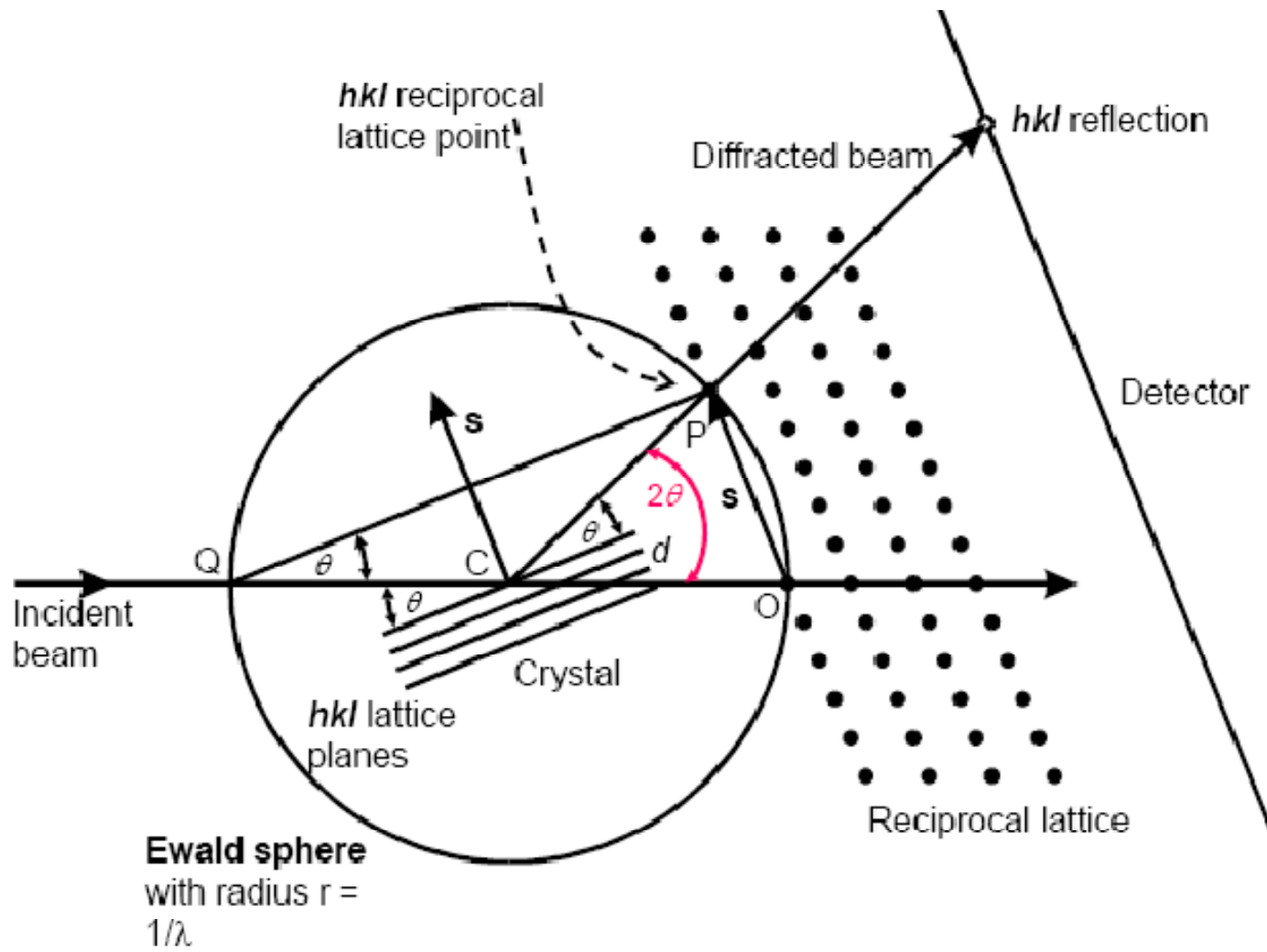
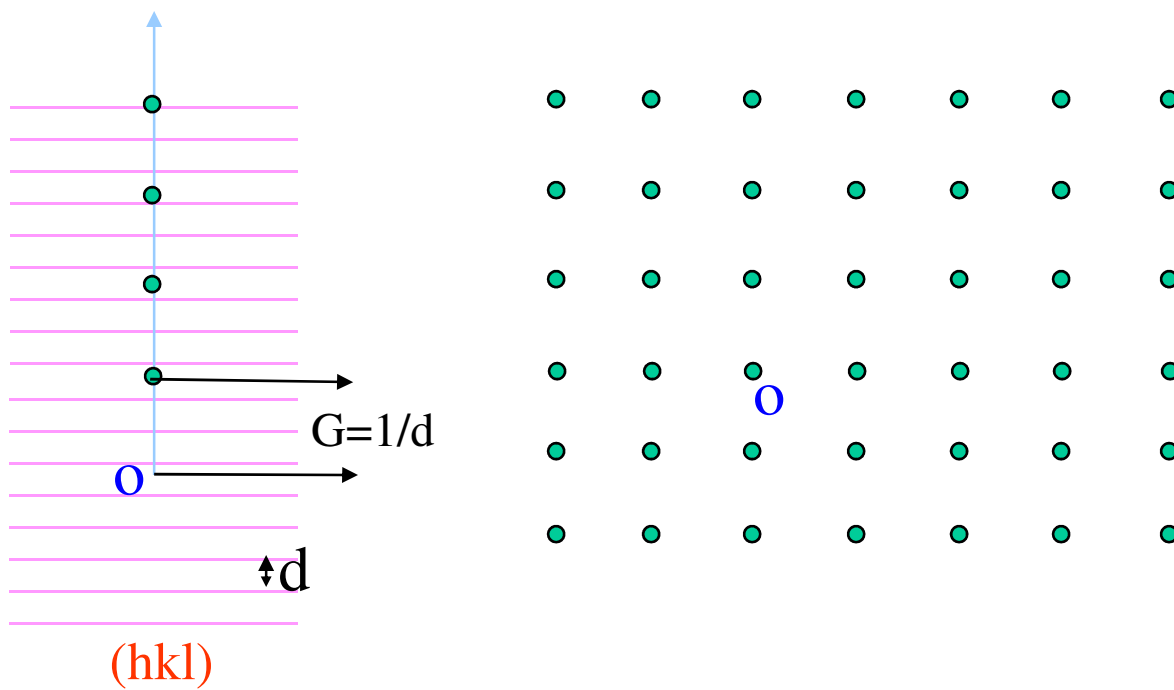


Figure 1: *Scattering of waves or particles with wavelength of roughly the same size as the lattice repeat distance allows us to learn about the lattice structure. Coherent addition of two particles or waves requires that $2d \sin \theta = \lambda$ (the Bragg condition), and yields a scattering maximum on a distant screen.*

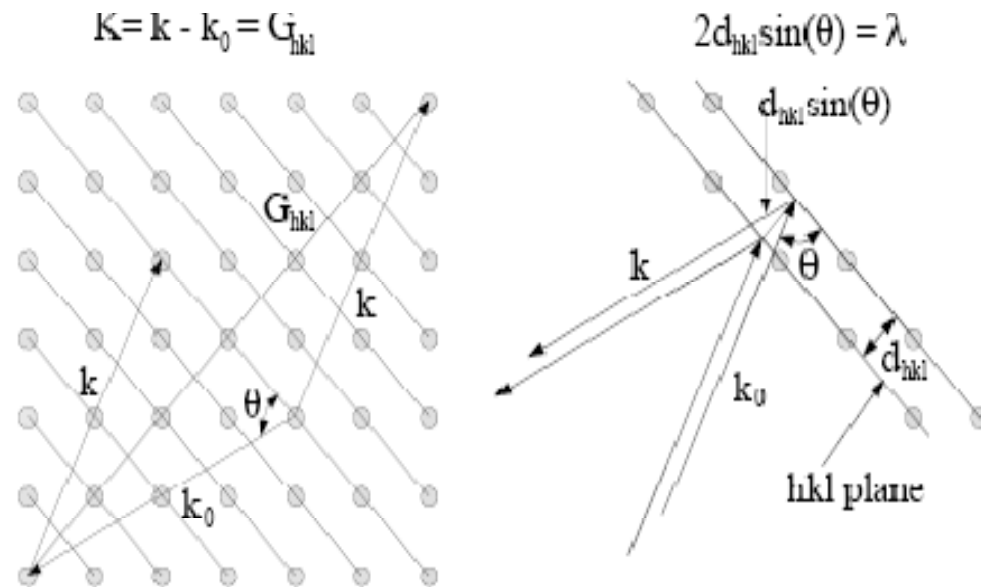
Ewald Construction



Reciprocal lattice construction



Bragg-Diffraction : Reciprocal Lattice

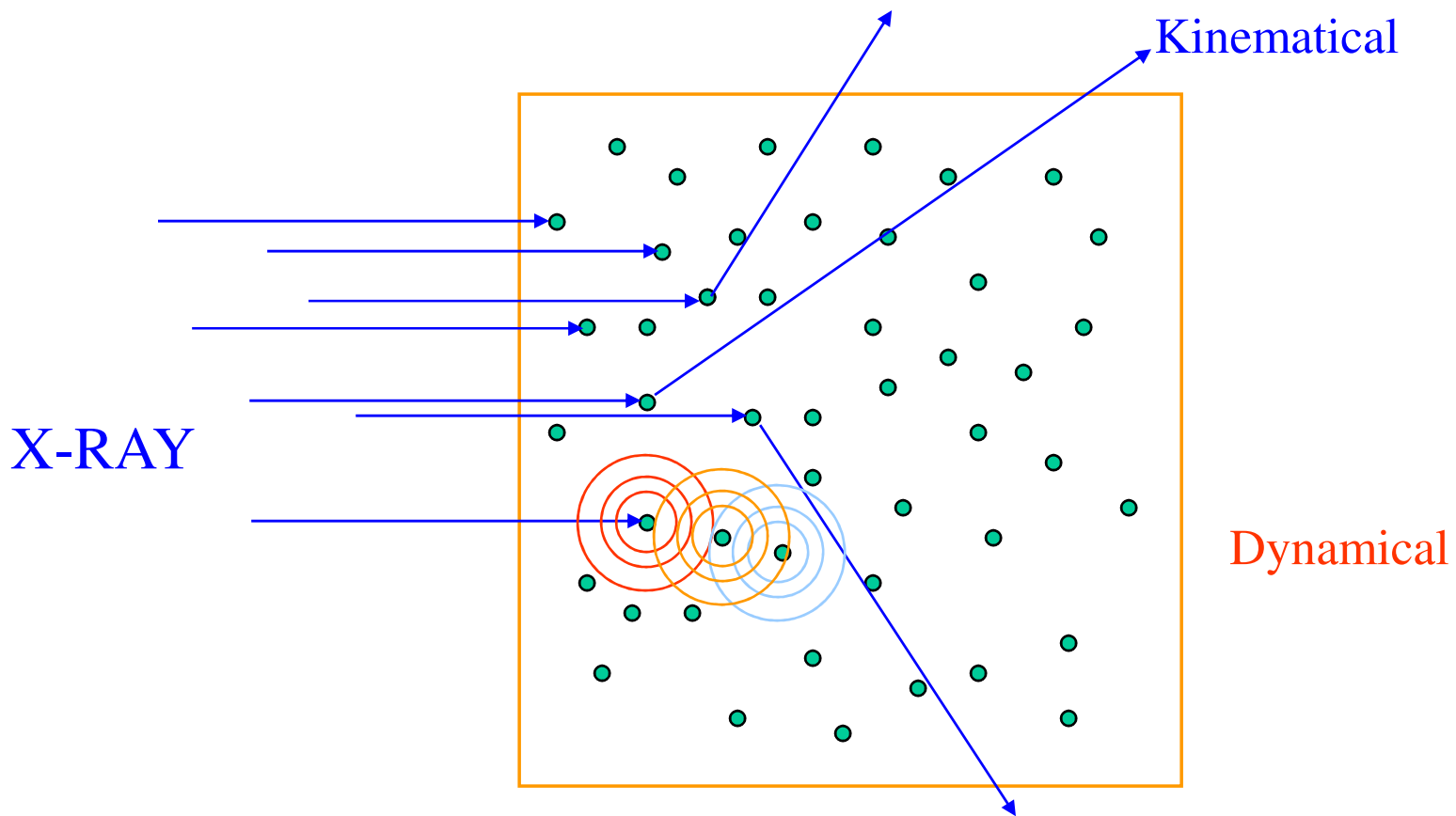


$$2d \sin\theta = \lambda$$

$$K_0 + G = K$$

$$k_0 = 1/\lambda$$

Scattering within the bulk

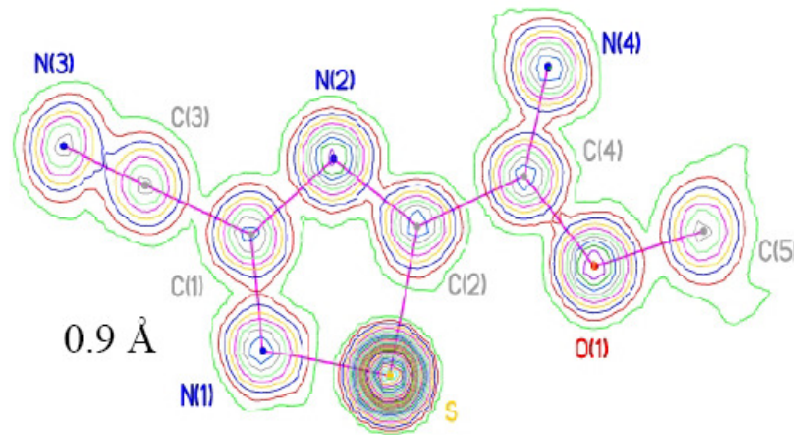


Kinematical-Scattering of X-rays

According to this approximation a x-ray once scattered does not get re-scattered by other scatterers in the bulk and the incident beam intensity(I_0) remains unaffected during the propagation of the beam in the bulk.

Intensity calculation based on this assumption matches very nicely with the experimentally measured intensity from real samples comprising “imperfect crystals” , small crystallites with defects

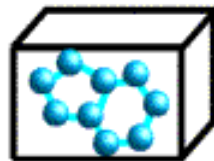
Hierarchy in scattering



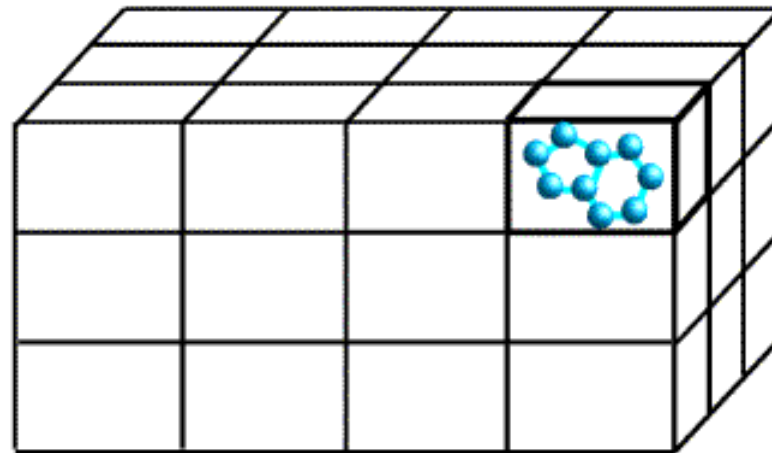
molecule



unit cell

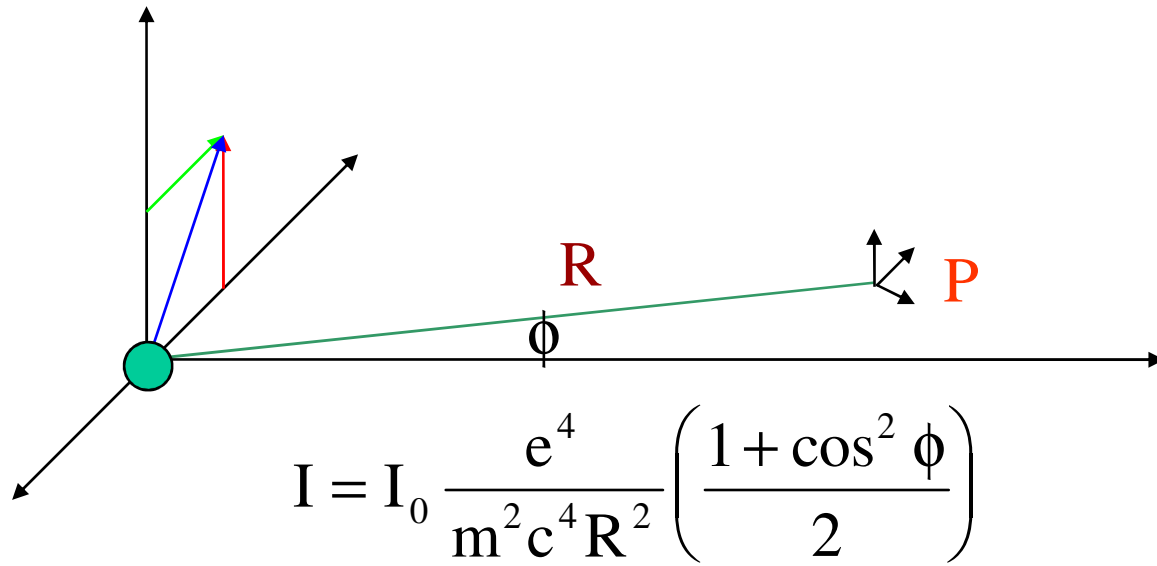


crystal



Electrons - Atom - Unit cell - Crystal

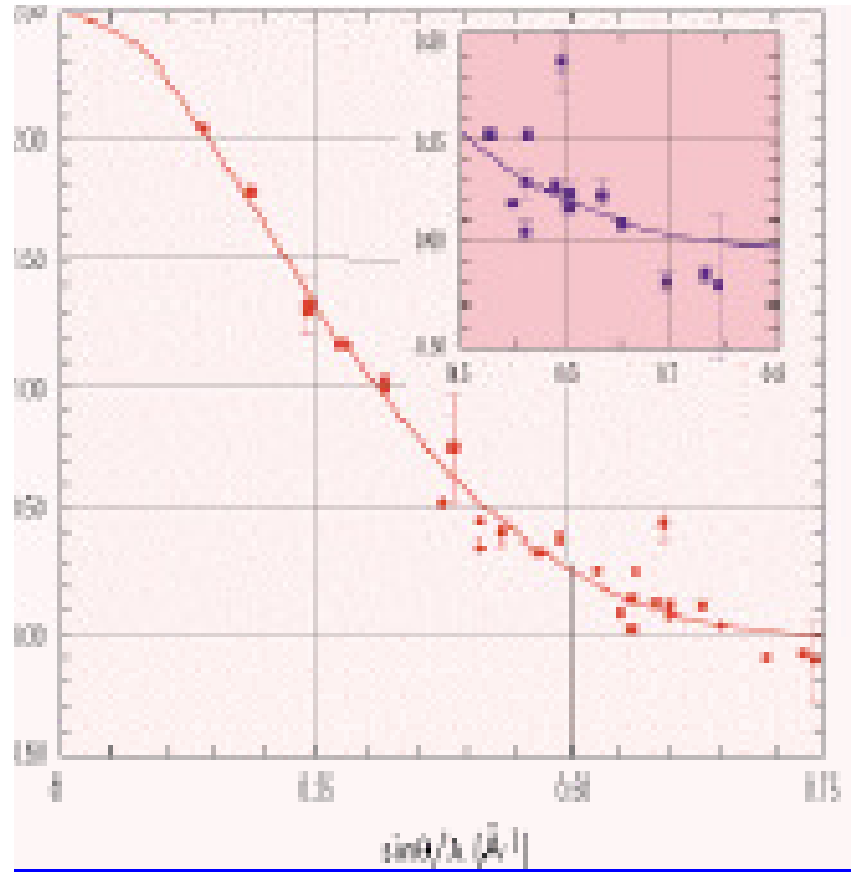
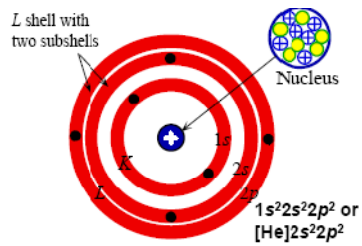
Thomson Scattering



$$I = I_0 \left(\frac{r_e}{R} \right)^2 p$$

$$r_e = \frac{e^2}{m c^2}$$

Atomic scattering Factor

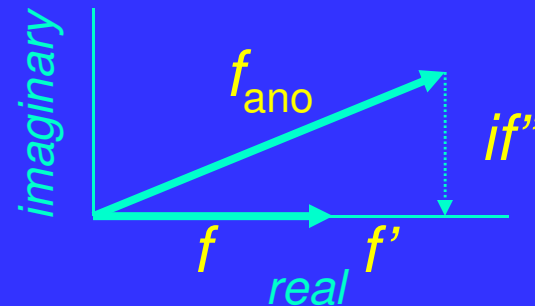


Multiple Anomalous Dispersion (MAD)

At the absorption edge of an atom, its scattering factor

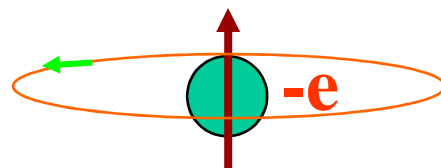
$$f_{\text{ano}} = f + f' + if''$$

Atom	f	f'	f''
Hg	80	-5.0	7.7
Se	34	-0.9	1.1



→ $F(h,k,l) = F(-h,-k,-l)$ → anomalous differences → positions of anomalous scatterers → Protein Phasing

Magnetic scattering



Since electrons not only have charge but also have spin and orbital angular momentum in an atom, these will couple with the electro-magnetic radiation and hence the magnetic atoms, together with charge form factors will also have magnetic form-factors too, which will give information on magnetic materials

$$\frac{\sigma_{mag}}{\sigma_{charge}} \cong \left(\frac{\hbar\omega}{mc^2} \right)^2 \frac{N_m^2}{N^2} \langle s \rangle^2 \frac{f_m^2}{f^2}$$

For Fe and x-rays of 10kV it will be

$$\frac{\sigma_{mag}}{\sigma_{charge}} \cong 4.10^{-6} \langle s \rangle^2$$

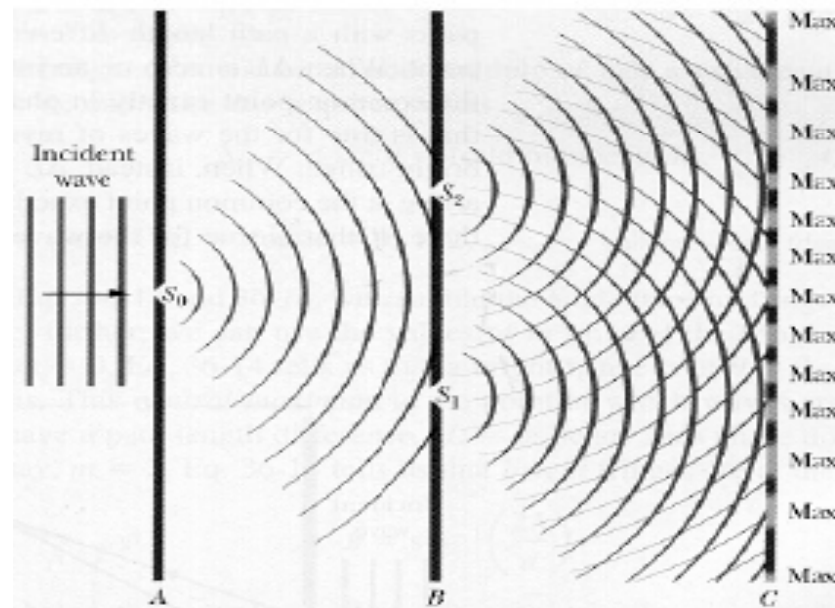
$$\frac{\sigma_{mag}}{\sigma_{charge}}$$

can be enhanced by using high energy and high intensity x-rays or by setting up resonance condition using tunable sources: **The Synchrotron**

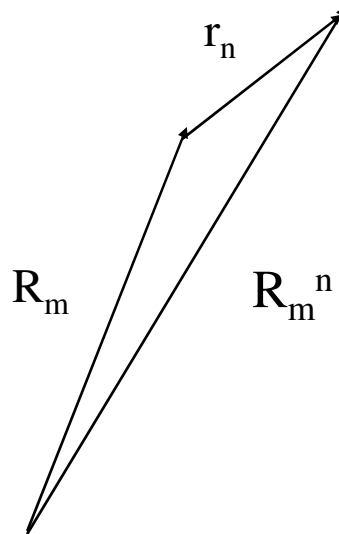
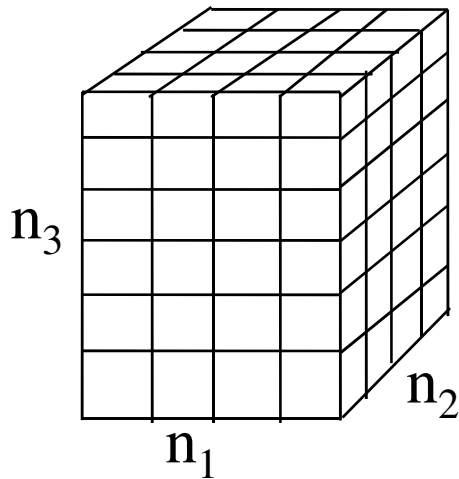
(1) M.Blume JAP 57(1),3615 (1985) and (2) D.Gibbons et.al PRL 61(10) 1241 (1988)

X-ray Diffraction - 1

Diffraction and interference of light



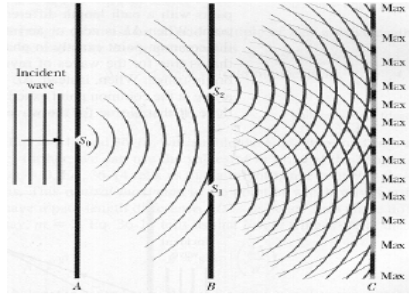
Scattering from small crystal: Kinematical treatment



$$\mathbf{R}_m = n_1 \mathbf{a}_1 + n_2 \mathbf{a}_2 + n_3 \mathbf{a}_3$$

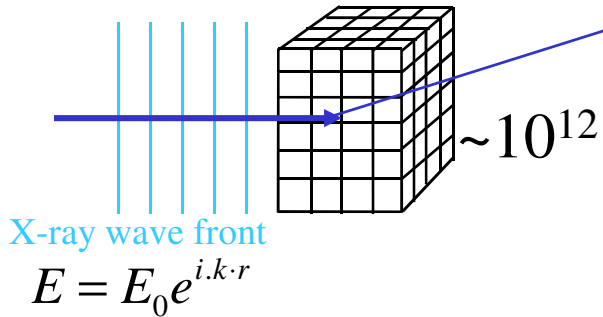
$$\mathbf{R}_m^n = \mathbf{R}_m + \mathbf{r}_n = n_1 \mathbf{a}_1 + n_2 \mathbf{a}_2 + n_3 \mathbf{a}_3 + \mathbf{r}_n$$

Scattered Amplitude



P

$$E_p = \sum E_p^n$$



$$E_p^n = \frac{E_0}{R} f_\theta e^{i\{\phi - (2\pi.k)[R - (S - S_0) \cdot (n_1 a_1 + n_2 a_2 + n_3 a_3 + r_n)]\}}$$

$$E_p = \frac{E_0}{R} e^{i(\phi - 2\pi R.k)} \sum_n f_\theta e^{2\pi i.k(s-s_0) \cdot r_n} \sum_{n_1}^{N_1-1} e^{2\pi i.k(s-s_0) \cdot n_1 \cdot a_1} \sum_{n_2}^{N_2-1} e^{2\pi i.k(s-s_0) \cdot n_2 \cdot a_2} \sum_{n_3}^{N_3-1} e^{2\pi i.k(s-s_0) \cdot n_3 \cdot a_3}$$

$$E_p = \sum E_p^n$$

$$E_p = \frac{E_0}{R} e^{i(\phi - 2\pi R \cdot k)} \sum_n f_\theta e^{2\pi i \cdot k (s - s_0) \cdot r_n} \sum_{n_1}^{N_1 - 1} e^{2\pi i \cdot k (s - s_0) \cdot n_1 \cdot a_1} \sum_{n_2}^{N_2 - 1} e^{2\pi i \cdot k (s - s_0) \cdot n_2 \cdot a_2} \sum_{n_3}^{N_3 - 1} e^{2\pi i \cdot k (s - s_0) \cdot n_3 \cdot a_3}$$

$$E_p^n = \frac{E_0}{R} f_\theta e^{i\{\phi - (2\pi \cdot k)[R - (S - S_0) \cdot (n_1 a_1 + n_2 a_2 + n_3 a_3 + r_n)]\}}$$

$$F(\theta) = \sum_n f_\theta e^{2\pi i \cdot k (s - s_0) \cdot r_n}$$

Amplitude contribution at each level

Scattering from Electron

$$I_e = I_0 \frac{e^4}{m^2 c^4 R^2} \left(\frac{1 + \cos^2 2\theta}{2} \right)$$

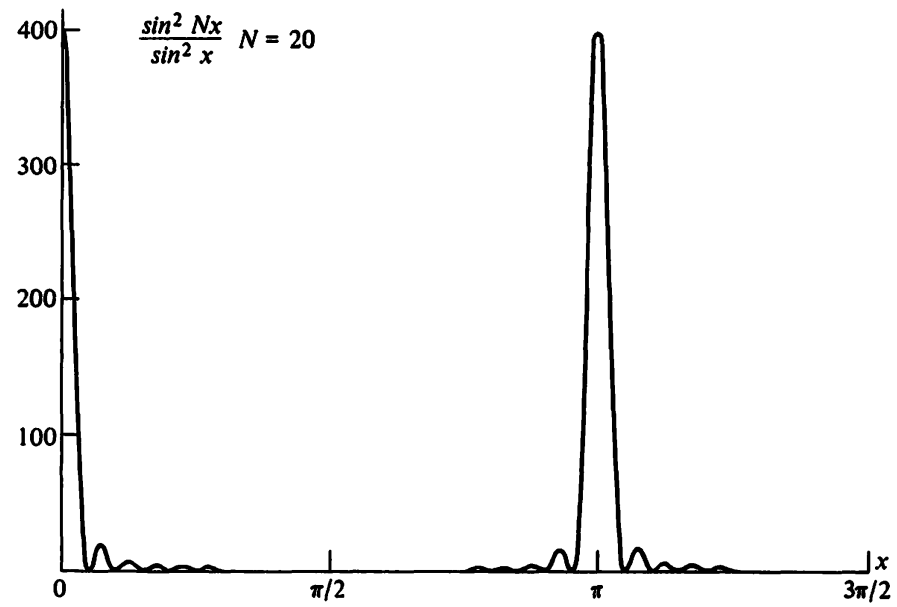
Scattered Amplitude from Unit cell

$$F = \sum_n f_n e^{2\pi i / \lambda (s - s_0) \cdot r_n}$$

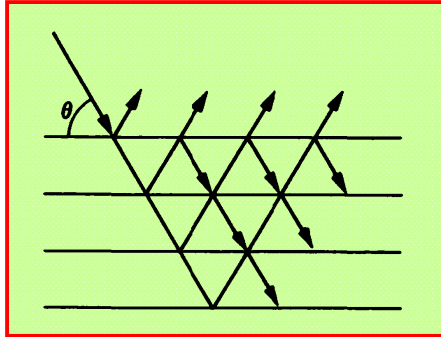
Scattered Intensity from a small Crystal with $N=(N_1 N_2 N_3)$ unit cells with a_1, a_2, a_3 lattice parameters

$$I_p = I_e F^2 \frac{\sin^2(\pi / \lambda)(s - s_0) \cdot N_1 a_1}{\sin^2(\pi / \lambda)(s - s_0) \cdot a_1} \frac{\sin^2(\pi / \lambda)(s - s_0) \cdot N_2 a_2}{\sin^2(\pi / \lambda)(s - s_0) \cdot a_2} \frac{\sin^2(\pi / \lambda)(s - s_0) \cdot N_3 a_3}{\sin^2(\pi / \lambda)(s - s_0) \cdot a_3}$$

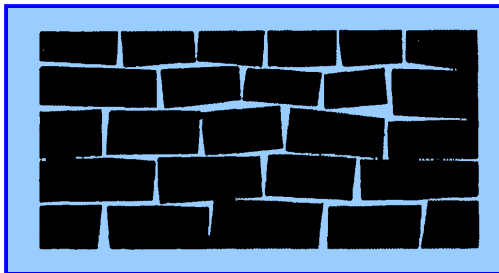
Lattice contribution



Extinction of Integrated intensity



Dynamical scattering $I_{\text{int}} \propto |F|$



Imperfect crystal: smaller the mosaic size
better the match between the observed and
kinematically approximated intensity

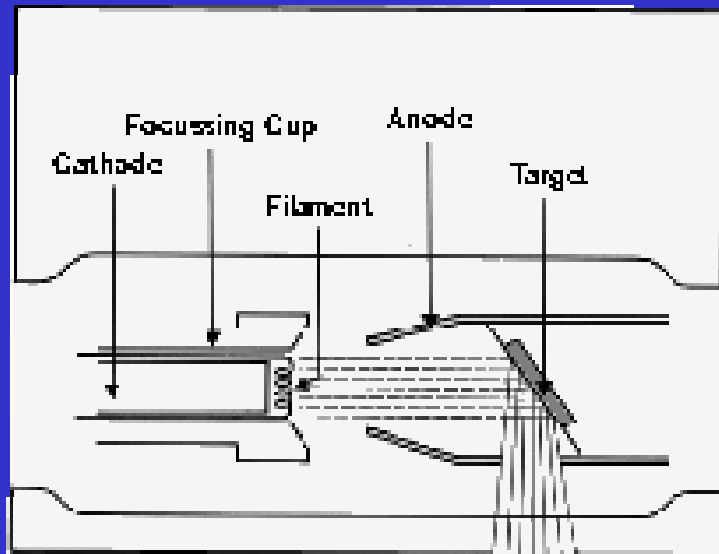
$$I_{\text{int}} \propto F^2$$

An Ideal imperfect crystal is not possible therefore some
Extinction always takes place even in usual powder samples

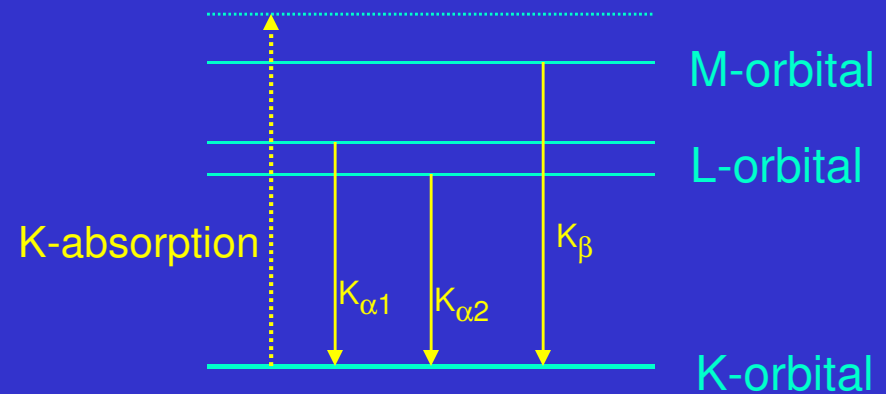
X-ray Instrumentation

X-ray Sources for Crystallographic Studies

Home Source – Rotating Anode



X-Ray Tube



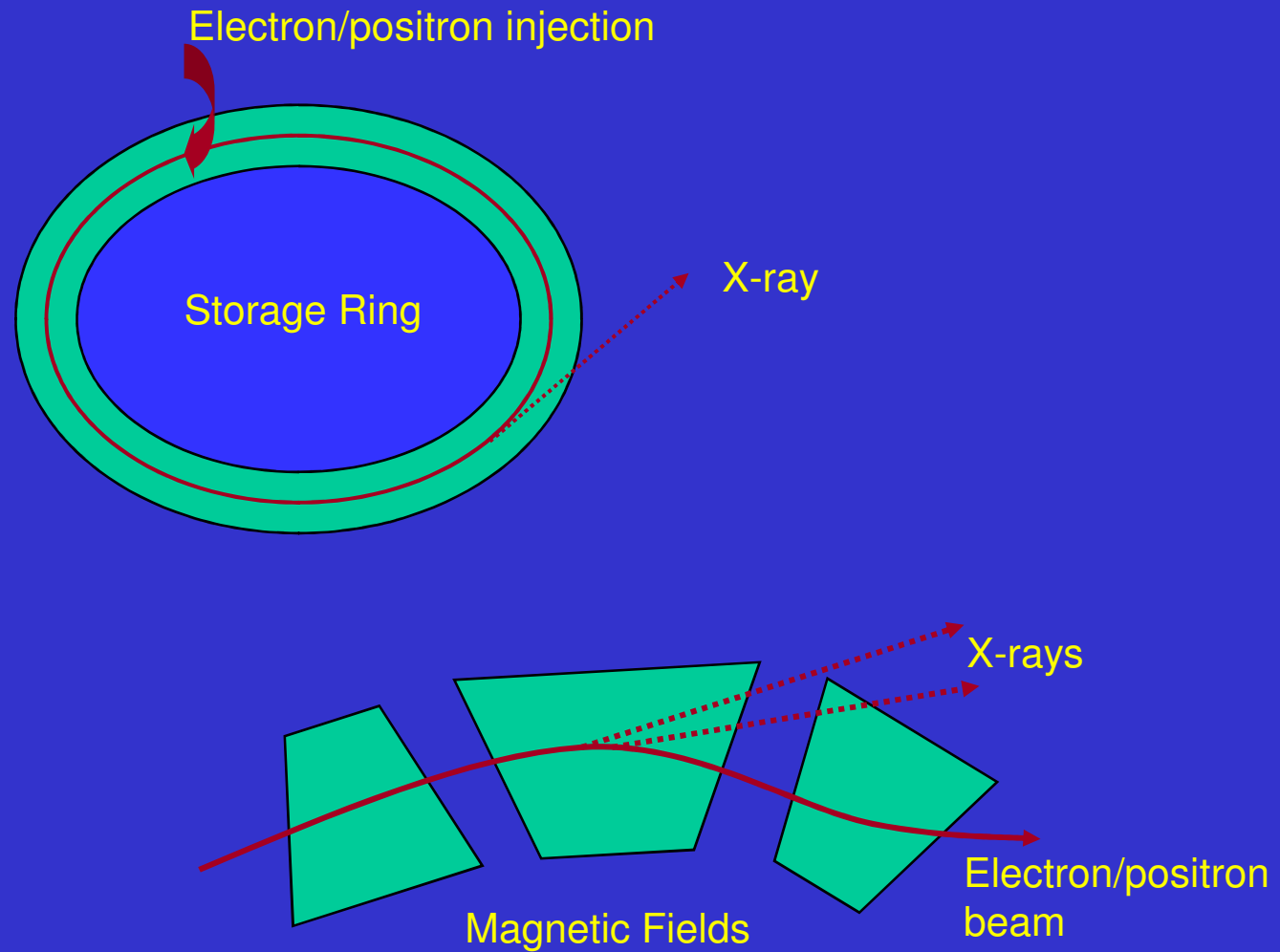
Wave-lengths

$$\text{Cu}(K_{\alpha 1}) = 1.54015 \text{ \AA}; \text{Cu}(K_{\alpha 2}) = 1.54433 \text{ \AA}$$

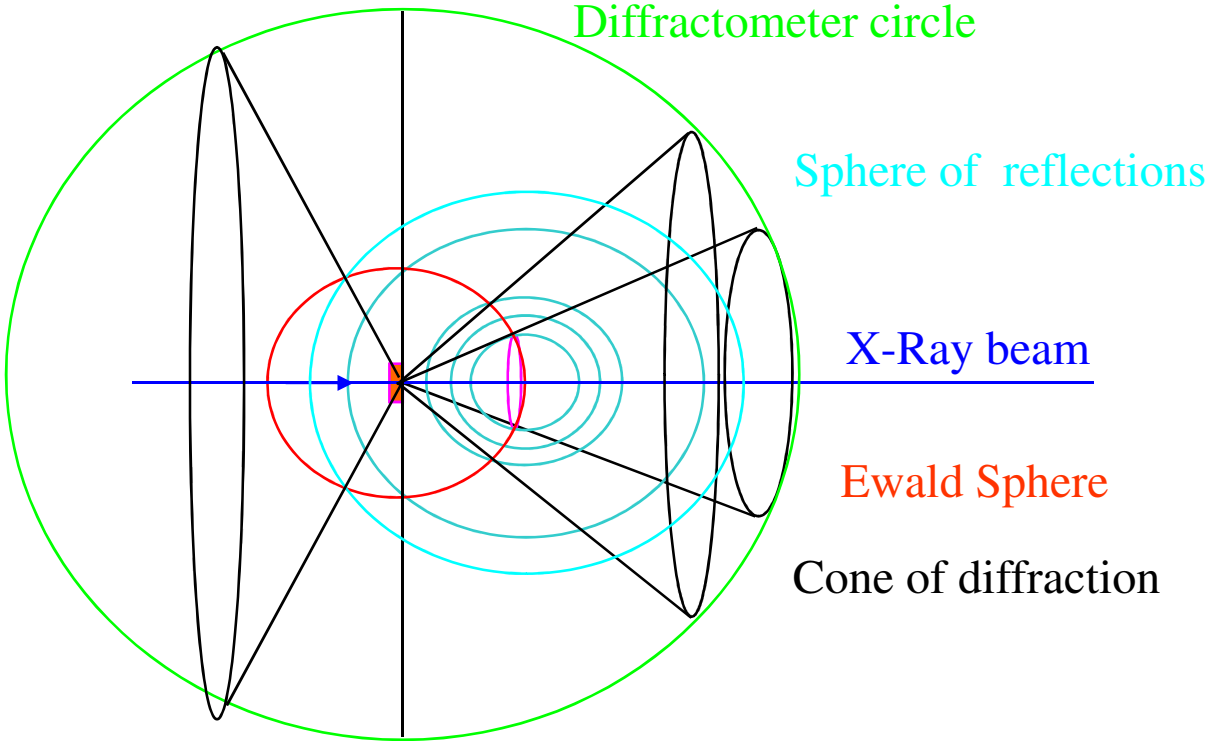
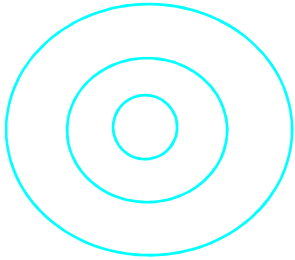
$$\text{Cu}(K_{\alpha}) = 1.54015 \text{ \AA}$$

$$\text{Cu}(K_{\beta}) = 1.39317 \text{ \AA}$$

Synchrotron X-rays



Reciprocal space of powder-sample



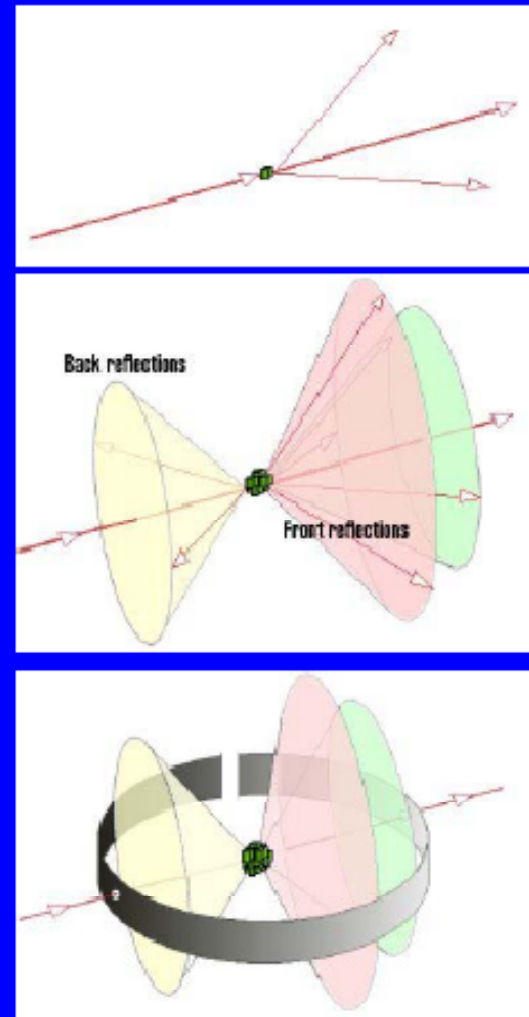
Example diffraction experiment: powder diffraction

Used to determine the value of the lattice parameters accurately.

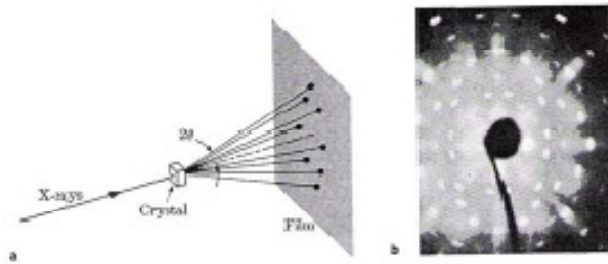
If a monochromatic x-ray beam is directed at a single crystal, then only one or two diffracted beams may result.

If the sample consists of some tens of randomly orientated single crystals, the diffracted beams lie on the surface of several cones.

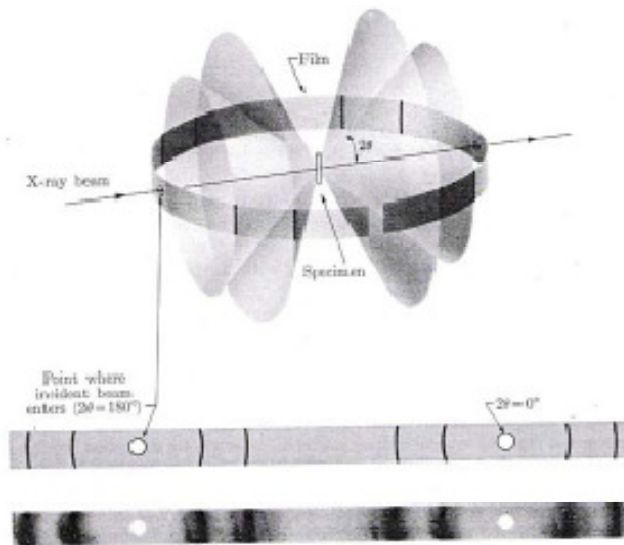
A sample of some hundreds of crystals (i.e. a powdered sample) show that the diffracted beams form continuous cones. Each cone intersects the film giving diffraction lines. For every set of crystal planes, by chance, one or more crystals will be in the correct orientation to give the correct Bragg angle to satisfy Bragg's equation. Each diffraction line is made up of a large number of small spots, each from a separate crystal.



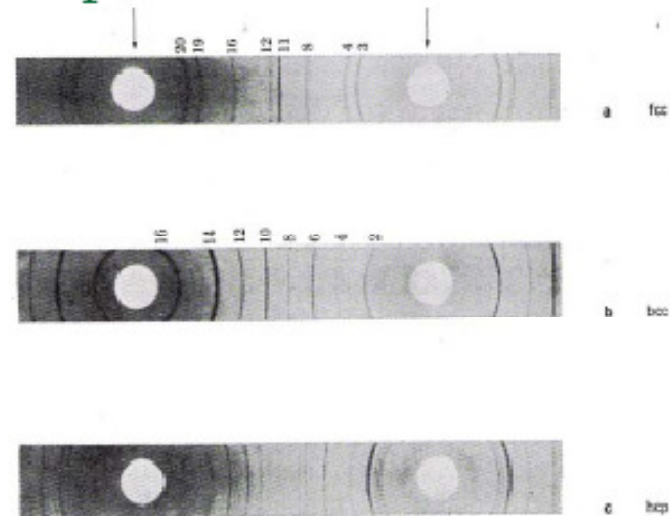
X-ray Diffraction – practical examples



5-23 Laue pattern. (a) Procedure. (b) Results. Each point on the film arises from a set of parallel crystal planes. (Courtesy of L. Thomson, The University of Michigan).



5-24 Powder pattern. Each diffraction line arises from a specific interplanar spacing. Through the use of monochromatic x-rays, the value of d_{hkl} may be calculated (Eq. 5-11). (Based on B. D. Cullity, Elements of X-ray Diffraction. Reading, Mass.: Addison-Wesley, 1956).



5-25 X-ray diffraction patterns for (a) copper, fcc; (b) tungsten, bcc; and (c) zinc, hcp. The numbers correspond to the values of $(h^2 + k^2 + l^2)$ in Table 5-4. Values of 2θ may be measured directly from the film arc. (Cl. Fig. 5-24.) (B. D. Cullity, Elements of X-ray Diffraction, Reading, Mass.: Addison-Wesley, 1956.)

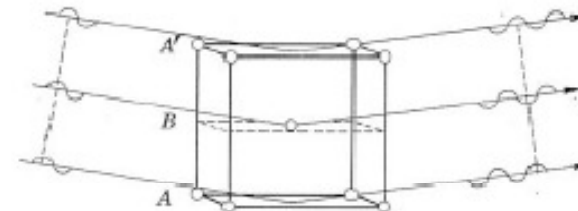
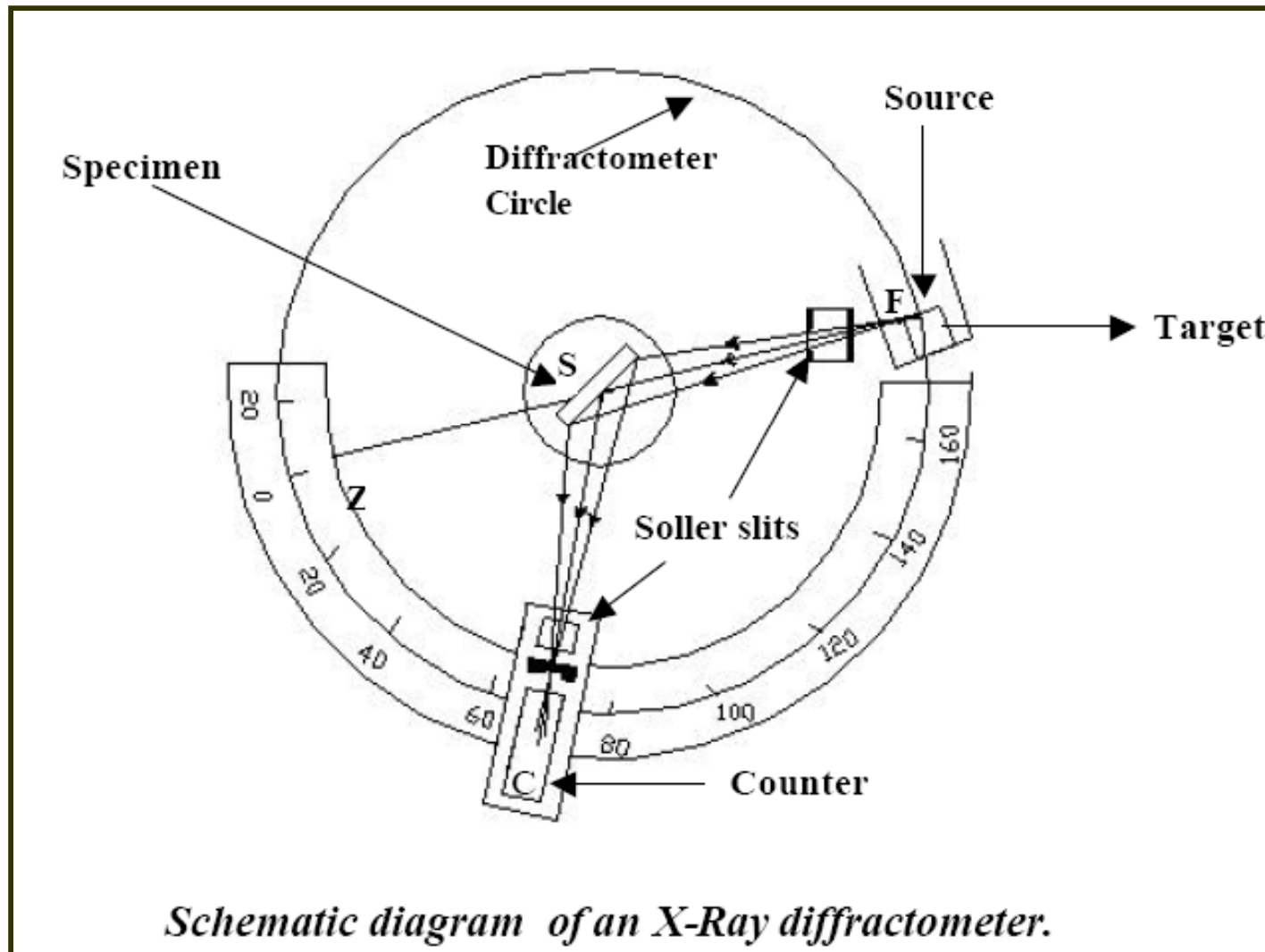
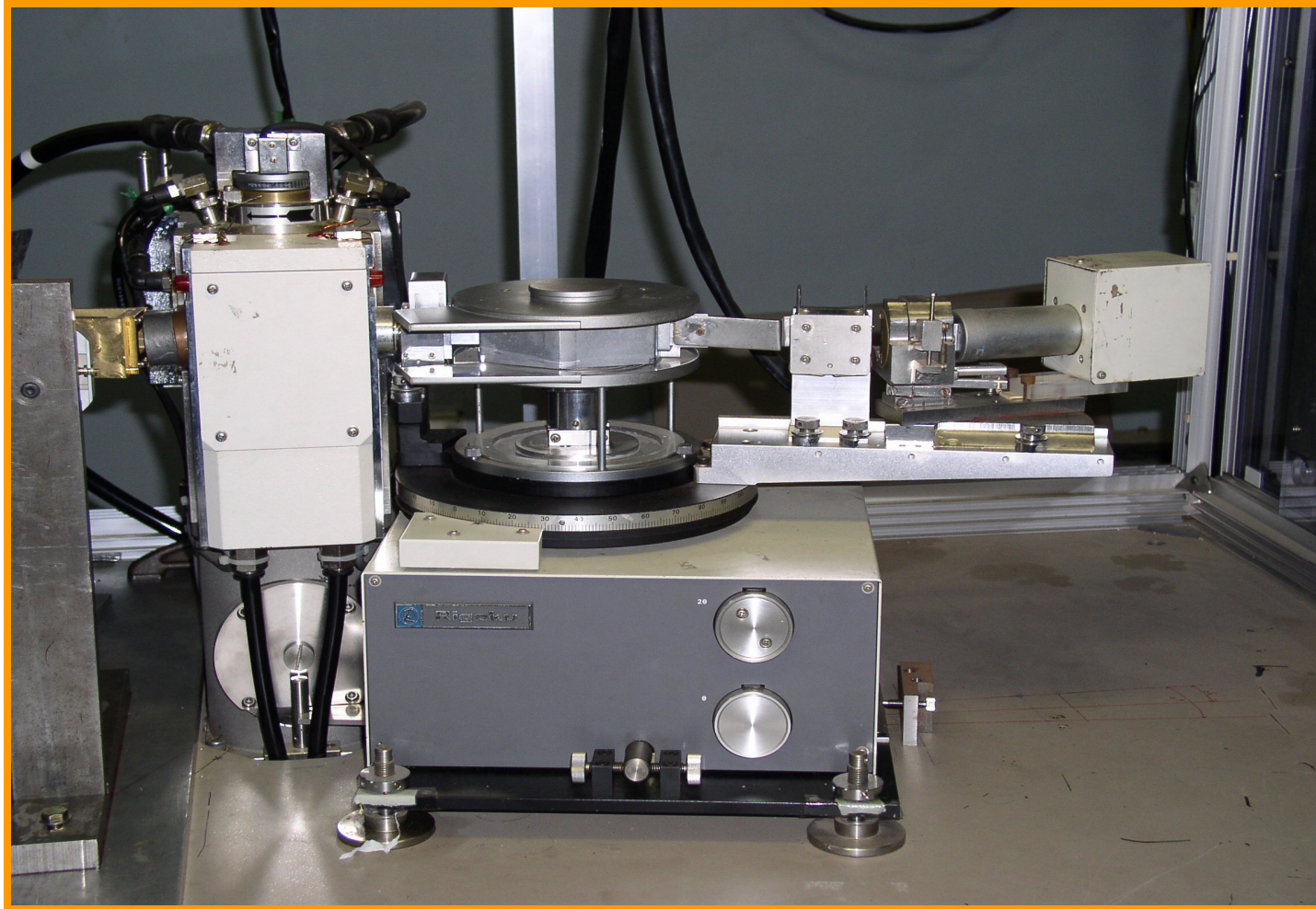


Fig. 4-7 Interference in 100 reflection from a b.c.c. lattice.

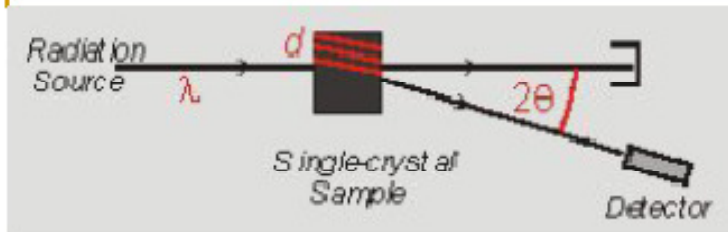
Geometry of a XRD-Goniometer



θ - 2θ X-ray Diffractometer (Rigaku)



X-ray Diffraction – practical examples - 2



Atomic form factor (f) – efficiency of an atom in scattering X-rays (f^2 gives of intensity scattered by an atom to the corresponding intensity from an electron).

The Structure factor (F) – amplitude of the sum of waves (sine waves of different amplitude and phase, but identical wavelength) scattered by each of the atoms in the unit cell. $|F|^2$ is the intensity of the observed reflection.

1912 - von Laue, Knipping, and Friedrich
the 1st experiment on X-ray diffraction

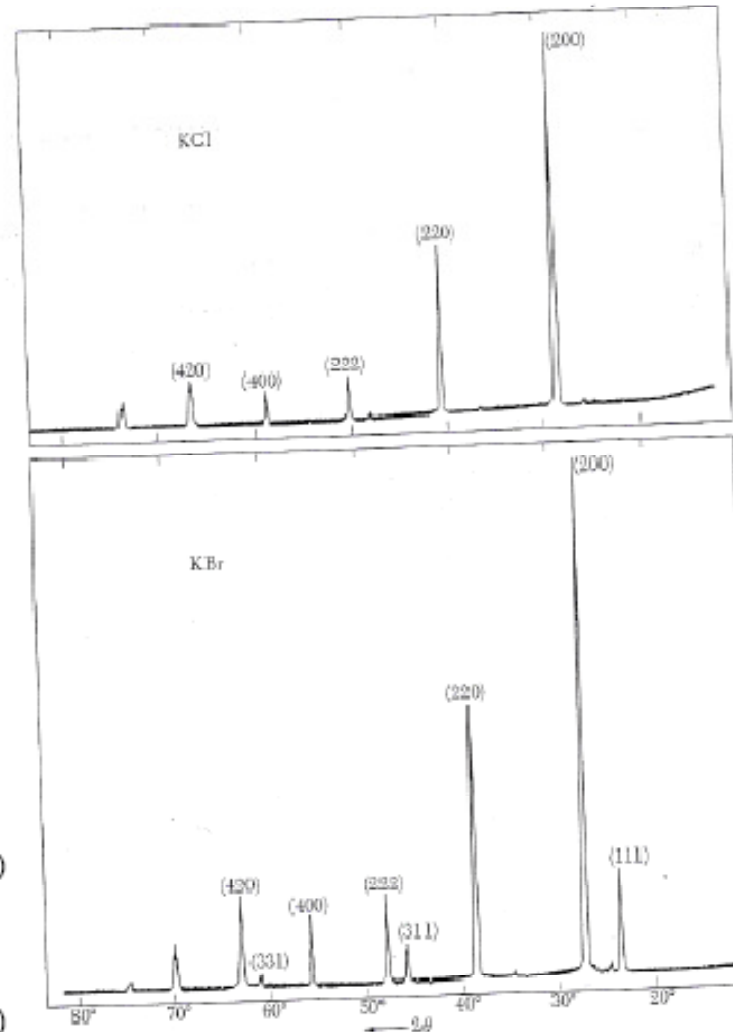
- el.-m. nature of X-rays
- the inner structure of crystals

(Nobel prize, 1914)

1913 - W. H. Bragg and W. L. Bragg
determined the KCl, NaCl, KBr, KI crystal structures

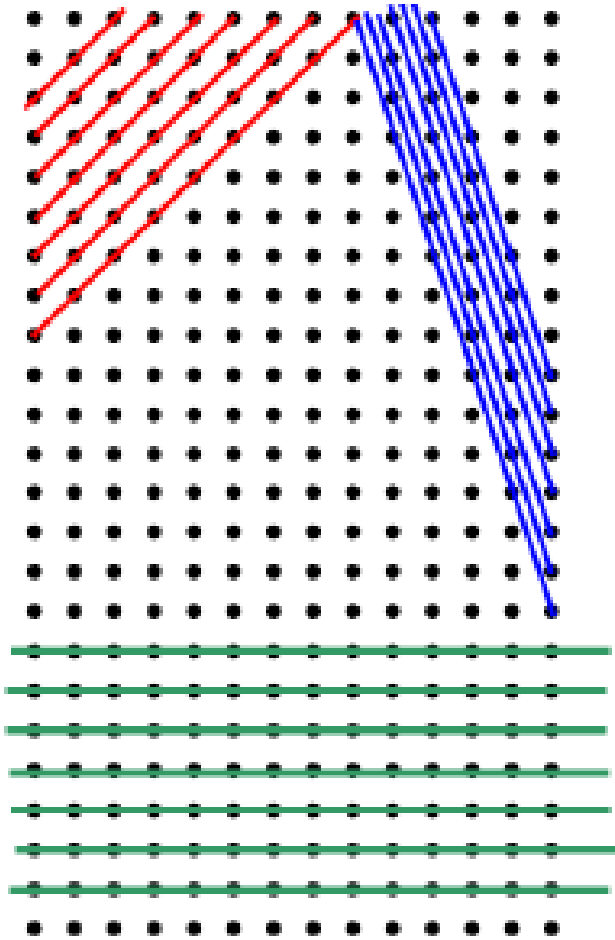
- X-ray crystallography

(Nobel prize, 1915)



Experimental Results

Analysis of the XRD data: Phase Analysis



Scattering Angle(2θ)	Interplaner Spacing(d -Å)	Relative Intensity
$2\theta_1$	d_1	I_1
$2\theta_2$	d_2	I_2
$2\theta_3$	d_3	I_3
$2\theta_4$	d_4	I_4
$2\theta_5$	d_5	I_5
$2\theta_6$	d_6	I_6
$2\theta_7$	d_7	I_7
$2\theta_8$	d_8	I_8
$2\theta_9$	d_9	I_9

ICDD data
base

Quick-
Phase
matching

$$F = \sum_n f_n e^{2\pi i / \lambda (s - s_0) \cdot r_n}$$

Analysis of the XRD data: Using Reitveld Refinement

Very accurate structural (like lattice parameters, Wyckoff positions of the atoms in the cell, thermal parameters) and microstructural (strain, shape and size) parameter can be obtained by fitting of the experimental XRD profile by multi parameter refinement of a given structural **MODEL**, under the constrain of a **space-group**.

This is accomplished by a computer program initially developed by Reitveld during his Ph.D. This works on the principle of least-square fitting of the data.

DOS, Windows Versions

The Rietveld Refinement

$$S_y = \sum w_i (y_i - y_{ci})^2$$

$w_i = 1/y_i$ y_i and y_{ci} are respectively the observed and calculated intensities at the i^{th} step.

$$y_{ci} = s \sum L_k |F_k|^2 \phi(2\theta_i - 2\theta_k) P_k A b + y_{bi} \quad \text{here}$$

s- scale factor, K-Miller indices, h, k, l for a Bragg reflection

L_k - Lorentz, polarization, and multiplicity factors

ϕ - Profile function

P_k - Preferred orientation function

A- The absorption factor

b-extinction

F_{k-S} structure factor for the K_{th} Bragg reflection

y_{bi} - The background intensity at the i_{th} step.

The Reliability Index

$$R_{wp} = \left[\frac{\sum_i w_i (y_{i(obs)} - y_{i(cal)})^2}{\sum_i w_i y_{i(obs)}^2} \right]^{1/2}$$

$$R_{exp} = \left[\frac{N - P}{\sum_i w_i y_{i(obs)}^2} \right]^{1/2}$$

$$R_B = \frac{100 \sum_i |y_{i(obs)} - y_{i(cal)}|}{\sum_i y_{i(obs)}}$$

$$S = \left[\frac{R_{wp}}{R_{exp}} \right]$$

$$\chi_v^2 = \left[\frac{R_{wp}}{R_{exp}} \right]^2 = S^2$$

Making of In-input File

COMM BaTiO3

! Files => DAT-file: BaTiO3, PCR-file: BaTiO3

!Job Npr Nph Nba Nex Nsc Nor Dum Iwg Ilo Ias Res Ste Nre Cry Uni Cor

0 5 1 0 0 0 0 0 0 0 0 0 1 0 0 0 0

!Ipr Ppl Ioc Mat Pcr Ls1 Ls2 Ls3 Syo Prf Ins Rpa Sym Hkl Fou Sho Ana

0 0 0 0 1 0 2 0 0 1 0 0 0 0 0 1 0!

!lambda1 Lambda2 Ratio Bkpos Wdt Cthm muR AsyLim Rpolarz

1.540590 1.544400 0.5000 70.0000 12.0000 0.7998 0.0000 30.00 0.0000

!NCY Eps R_at R_an R_pr R_gl Thmin Step Thmax PSD Sent0

20.01 0.39 0.39 0.39 0.39 20.0000 0.0200 120.0000 0.000 0.000!

20 !Number of refined parameters

Zero Code Sycos Code Sysin Code Lambda Code MORE

-0.0623 21.00 0.0000 0.00 0.0298 141.00 0.000000 0.00 0

Background coefficients/codes

4.6616 0.46056 0.30445E-01 -8.1480 11.984 0.00000

31.000 41.000 51.000 61.000 71.000 0.000

Data for PHASE number: 1 ==> Current R_Bragg: 5.61

!-----

BaTiO3

!Nat Dis Mom Pr1 Pr2 Pr3 Jbt Irf Isy Str Furth ATZ Nvk Npr More

4 0 0 0.0 0.0 1.0 0 0 0 0 0 0.00 0 5 0

P 4 M M <--Space group symbol

!Atom Typ X Y Z Biso Occ In Fin N_t /Codes

Ba Ba+2 0.00000 0.00000 0.00000 0.00000 0.12500 0 0 0

0.00 0.00 0.00 0.00 0.00

Ti Ti+4 0.50000 0.50000 0.51857 0.00000 0.12500 0 0 0

0.00 0.00 160.00 0.00 0.00

O1 O-2 0.50000 0.50000 0.00000 0.00000 0.12500 0 0 0

0.00 0.00 0.00 0.00 0.00

O2 O-2 0.50000 0.00000 0.51272 0.00000 0.25000 0 0 0

0.00 0.00 151.00 0.00 0.00

Scale Shape1 Bov Str1 Str2 Str3 Strain-Model

0.12649E-02 0.2111 -0.3431 0.0000 0.0000 0.0000 0

11.00000 131.00 171.00 0.00 0.00 0.00

U V W X Y GauSiz LorSiz Size-Model

0.02535 -0.02246 0.01610 0.00583 0.00000 0.00000 0.00000 0

111.00 121.00 101.00 181.00 0.00 0.00 0.00

a b c alpha beta gamma

3.993804 3.993804 4.029977 90.000000 90.000000 90.000000

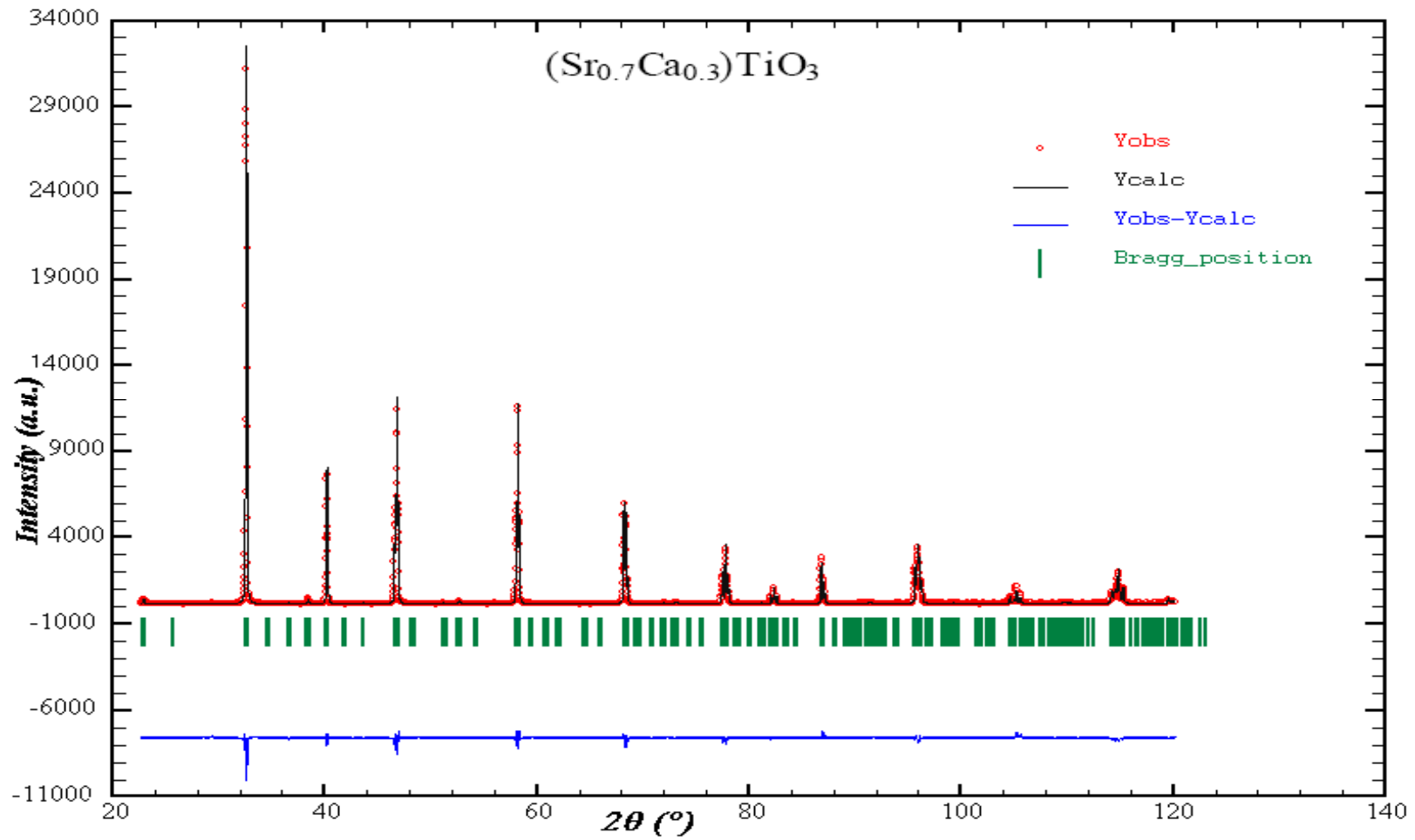
81.00000 81.00000 91.00000 0.00000 0.00000 0.00000

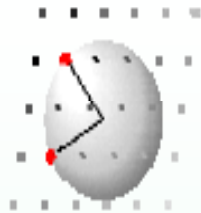
! Pref1 Pref2 Asy1 Asy2 Asy3 Asy4

0.00000 0.00000 0.14705 0.07978 0.00000 0.00000

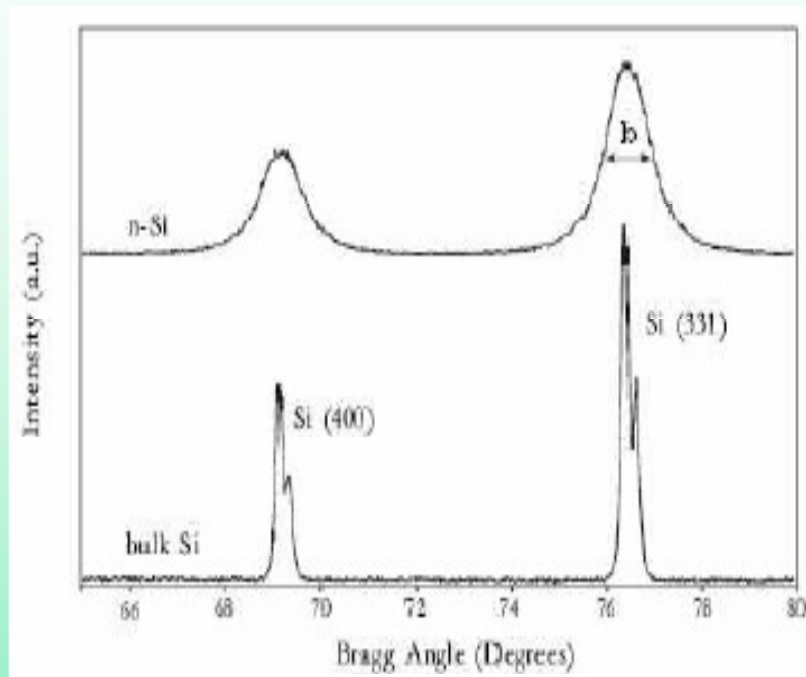
0.00 0.00 191.00 201.00 0.00 0.00

Reitveld Refinement of (SrCa)TiO₃





Sizes of nanocrystals



Scherrer formula:

the intrinsic peak width B (in radian) due to particle size is D

$$D = \frac{0.9 \lambda}{B \cos \theta}$$

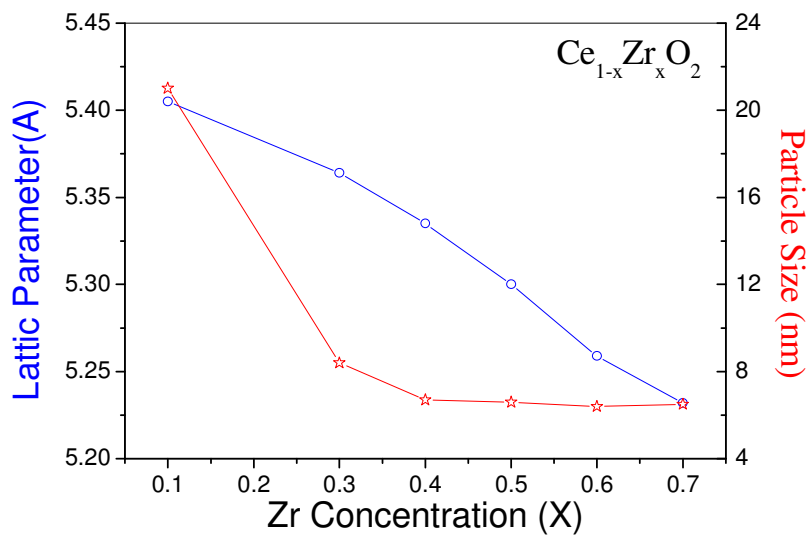
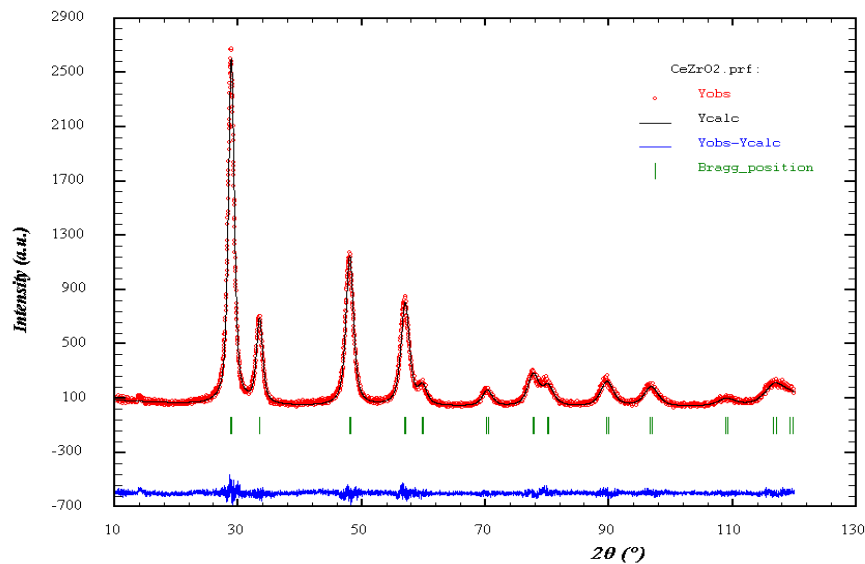
$$B = 0.019 \text{ rad}$$

$$\lambda = 1.54 \text{ \AA}$$

$$\theta = 38.2^\circ$$

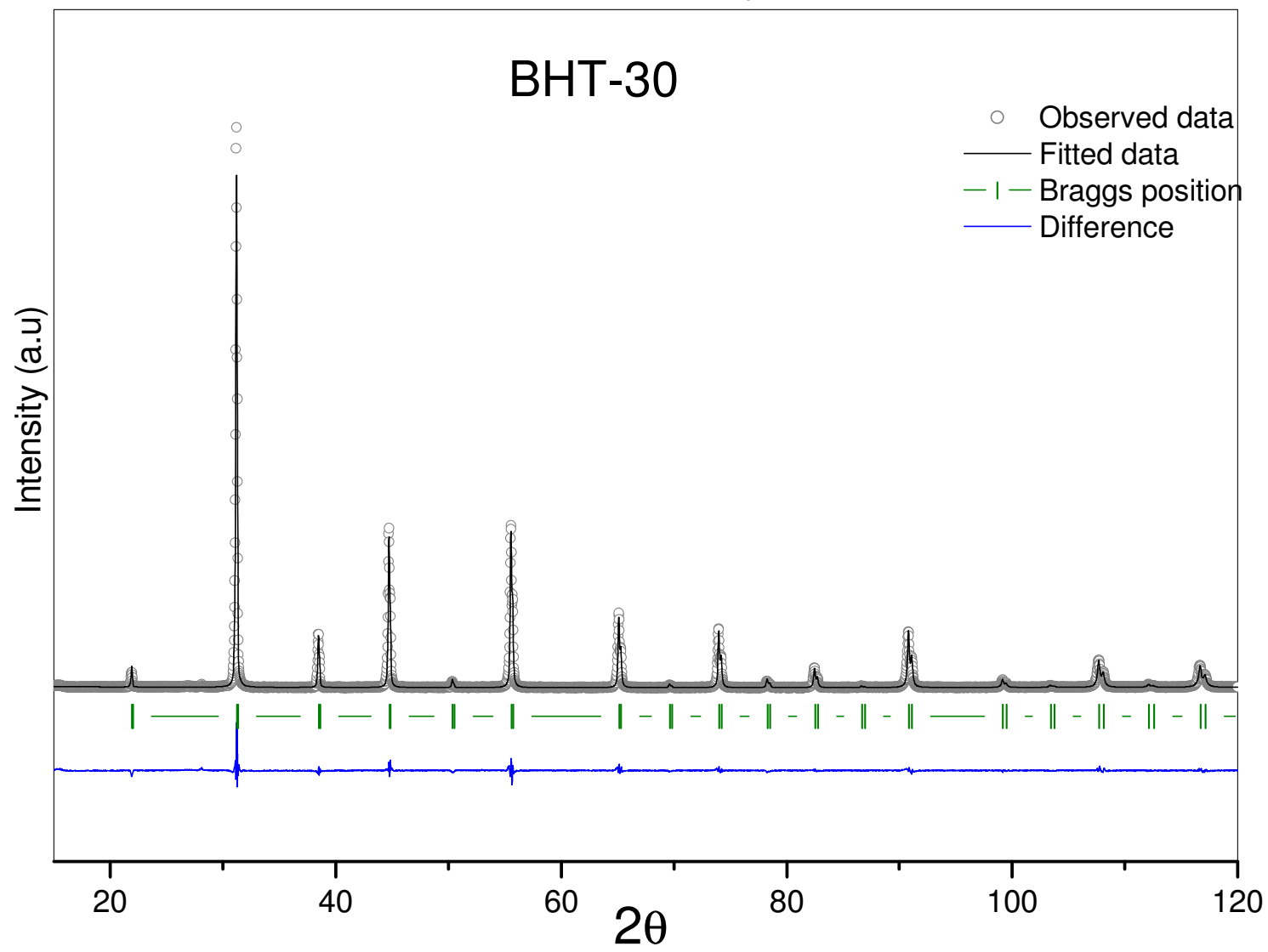
$$D \approx 100 \text{ \AA}$$

Ce7Zr3O2

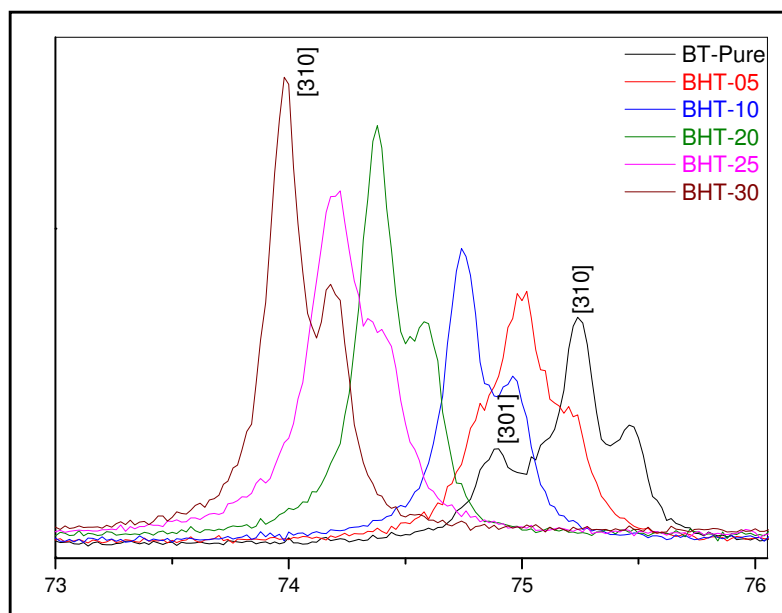


Composition	Lattice parameter (Å)	Particle size (nm)
Ce_{0.9}Zr_{0.1}O₂	5.405	21
Ce_{0.7}Zr_{0.3}O₂	5.364	8.4
Ce_{0.6}Zr_{0.4}O₂	5.335	6.7
Ce_{0.5}Zr_{0.5}O₂	5.300	6.6
Ce_{0.4}Zr_{0.6}O₂	5.259	6.4
Ce_{0.3}Zr_{0.7}O₂	5.232	6.5

Reitveld Refinement analysis of BaTiHfO₃



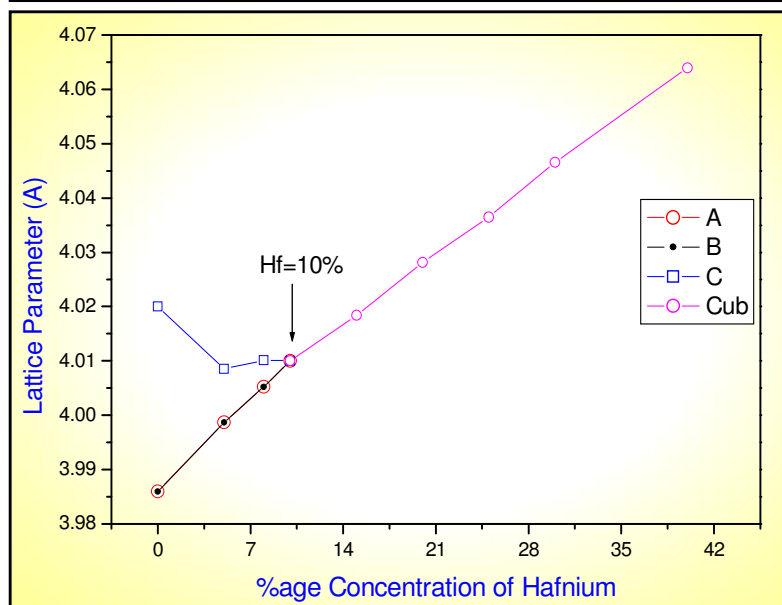
Tetragonal to Cubic transition with increasing Hf in $\text{Ba}(\text{Ti}_{1-x}\text{Hf}_x)\text{O}_3$



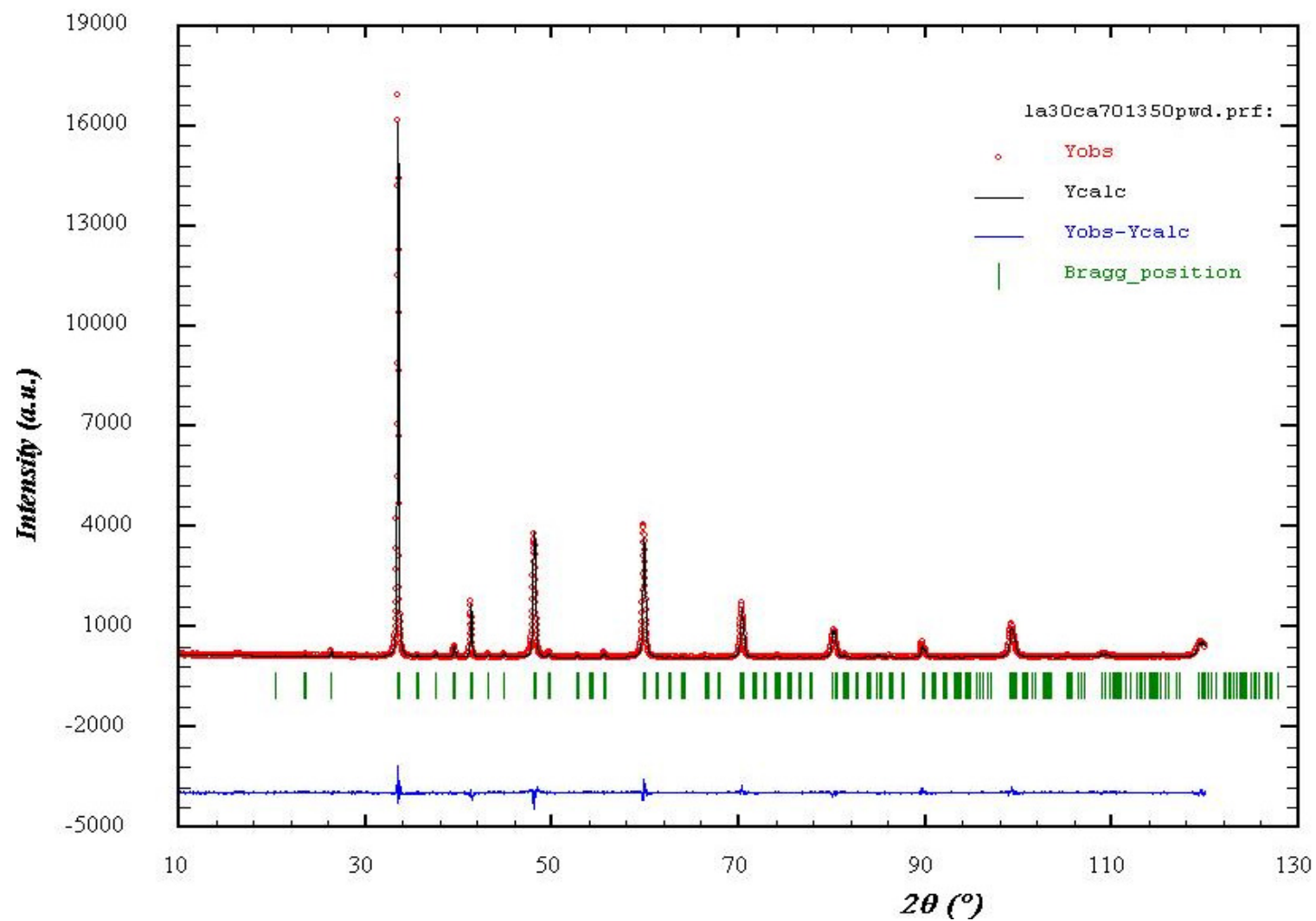
Ionic Radius

Hf^{4+} 0.71Å

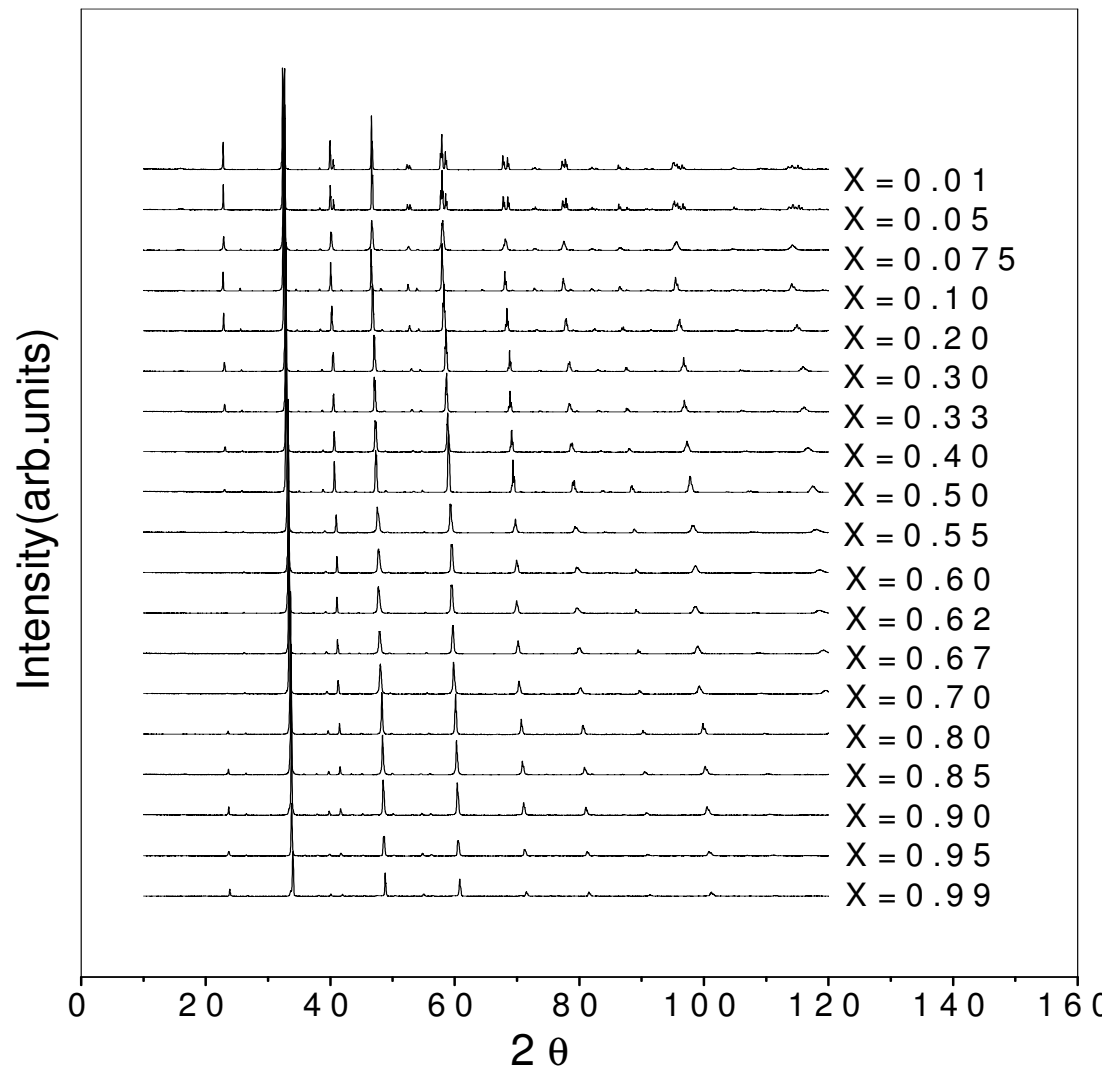
Ti^{4+} 0.605Å



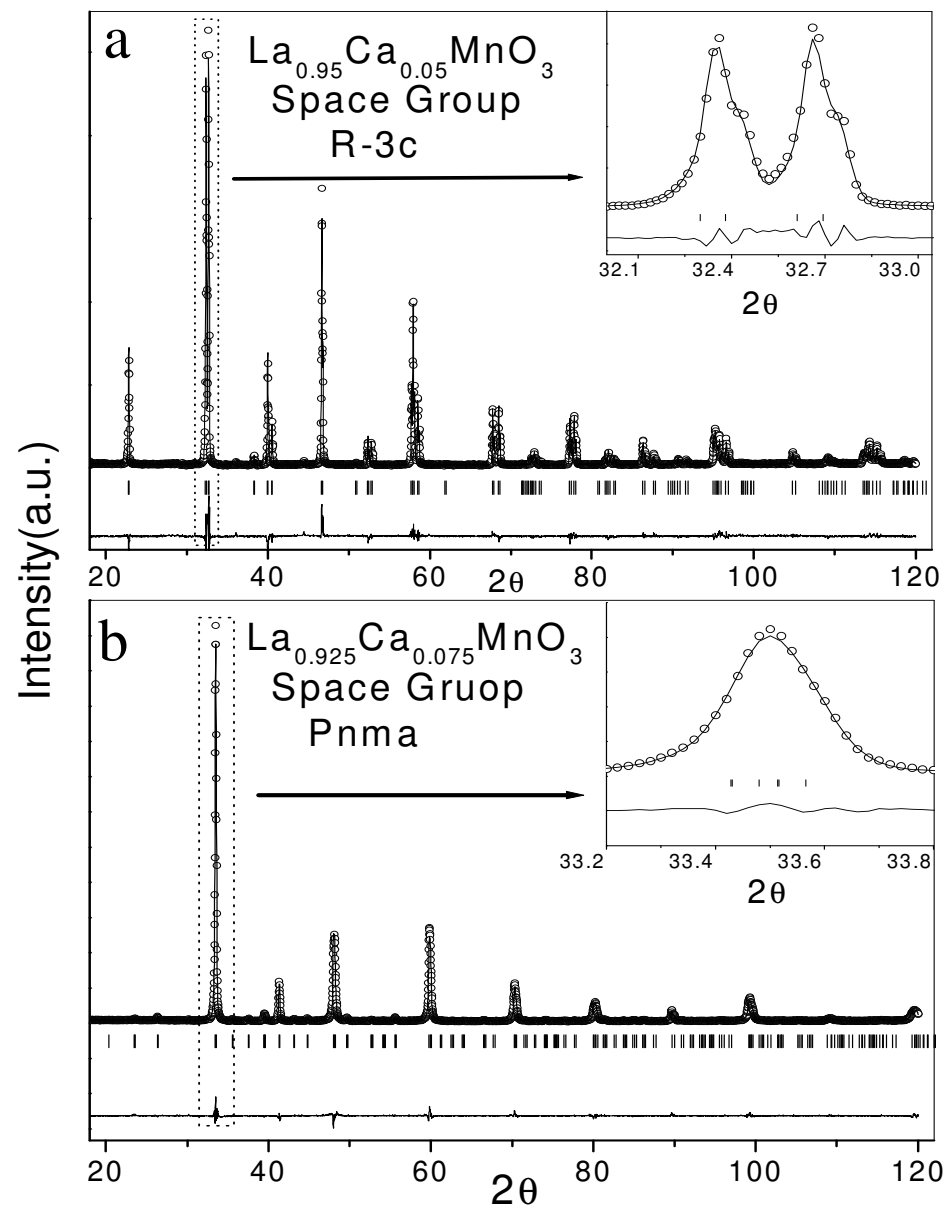
Rietveld Refinement of $\text{La}_{0.30}\text{Ca}_{0.70}\text{MnO}_3$



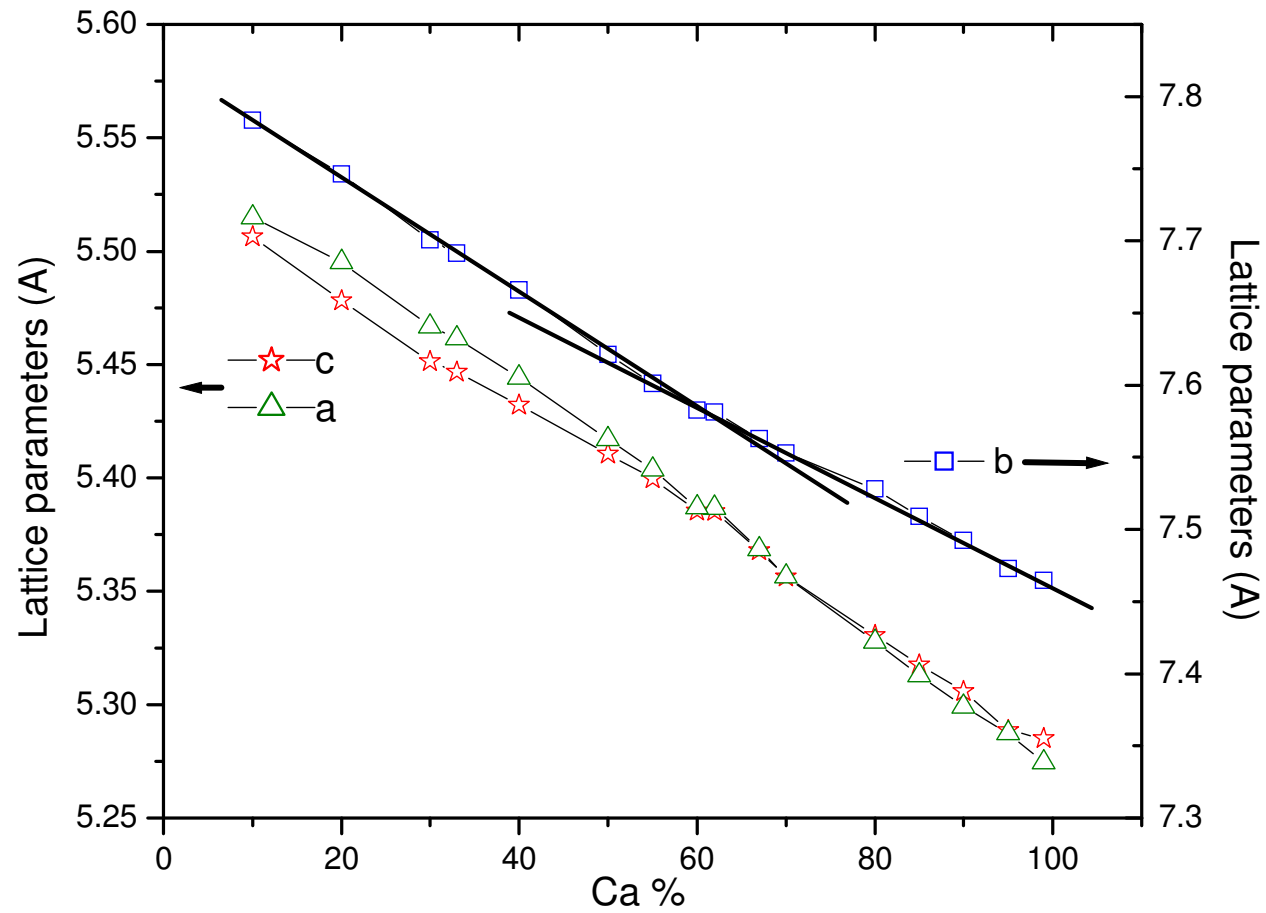
Powder XRD for $\text{La}_{1-x}\text{Ca}_x\text{MnO}_3$ for $(0.01 \leq x \leq 1)$



Structural Phase Transformation in $\text{La}_{1-x}\text{Ca}_x\text{MnO}_3$



Variation of Lattice parameters with doping concentration.

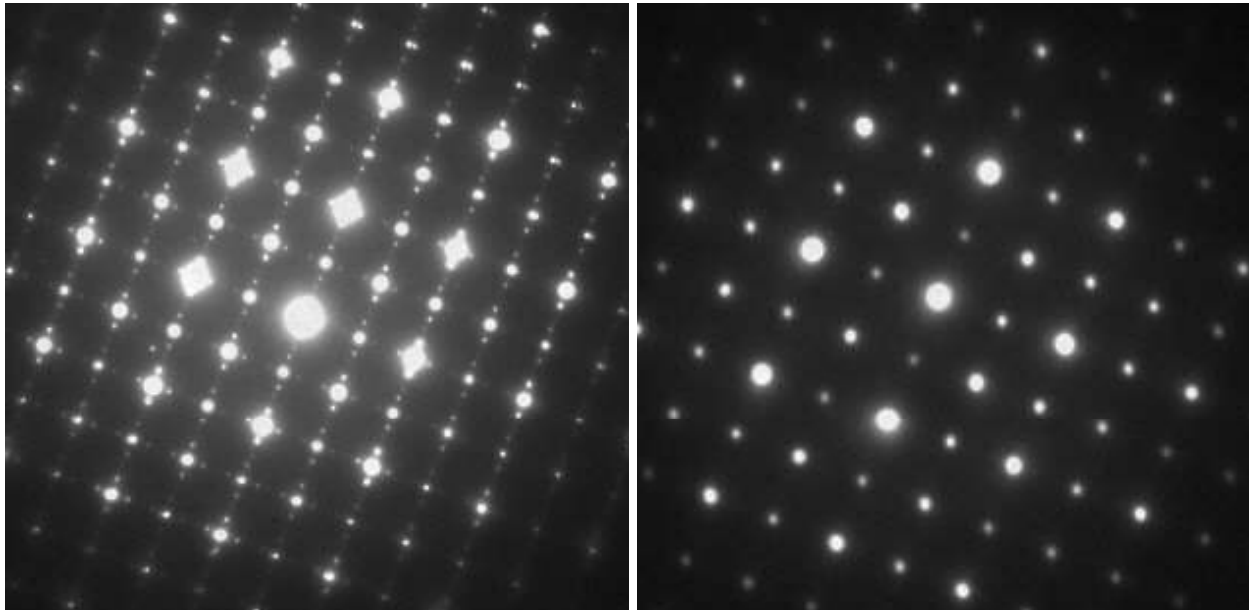


Low-temperature XRD Studies



Down to 90K

Phase coexistence of CO and a Monoclinic phase

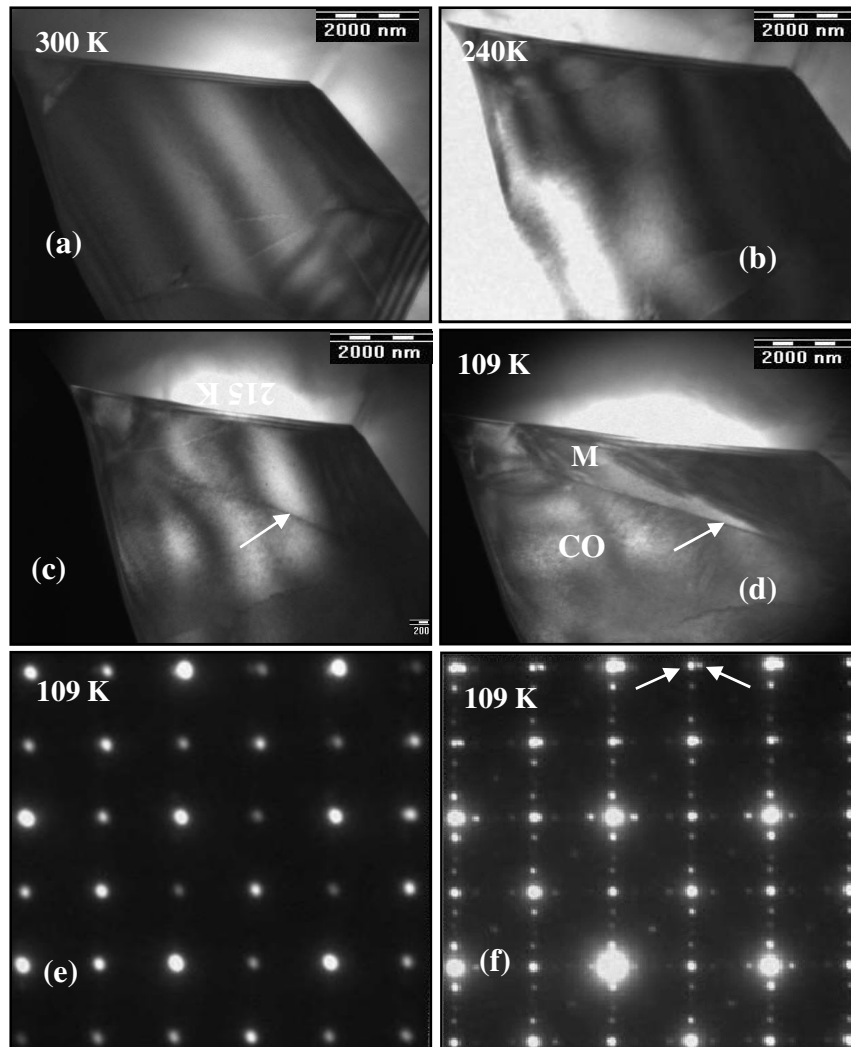


Charge-Ordered phase (150K)

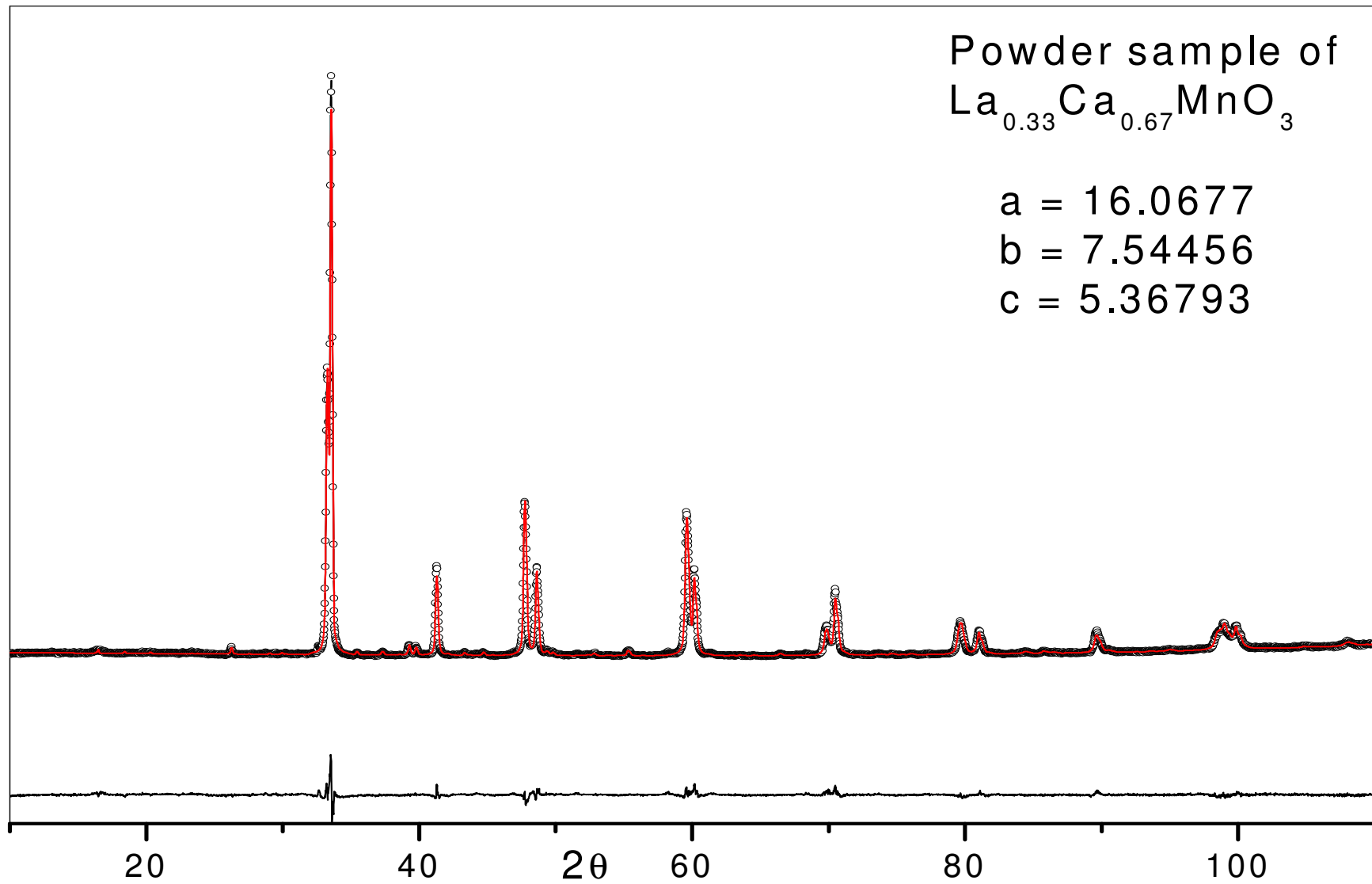
Monoclinic phase (150K)

J.C.Loudon et.al PRB 71,220408(R) (2005)

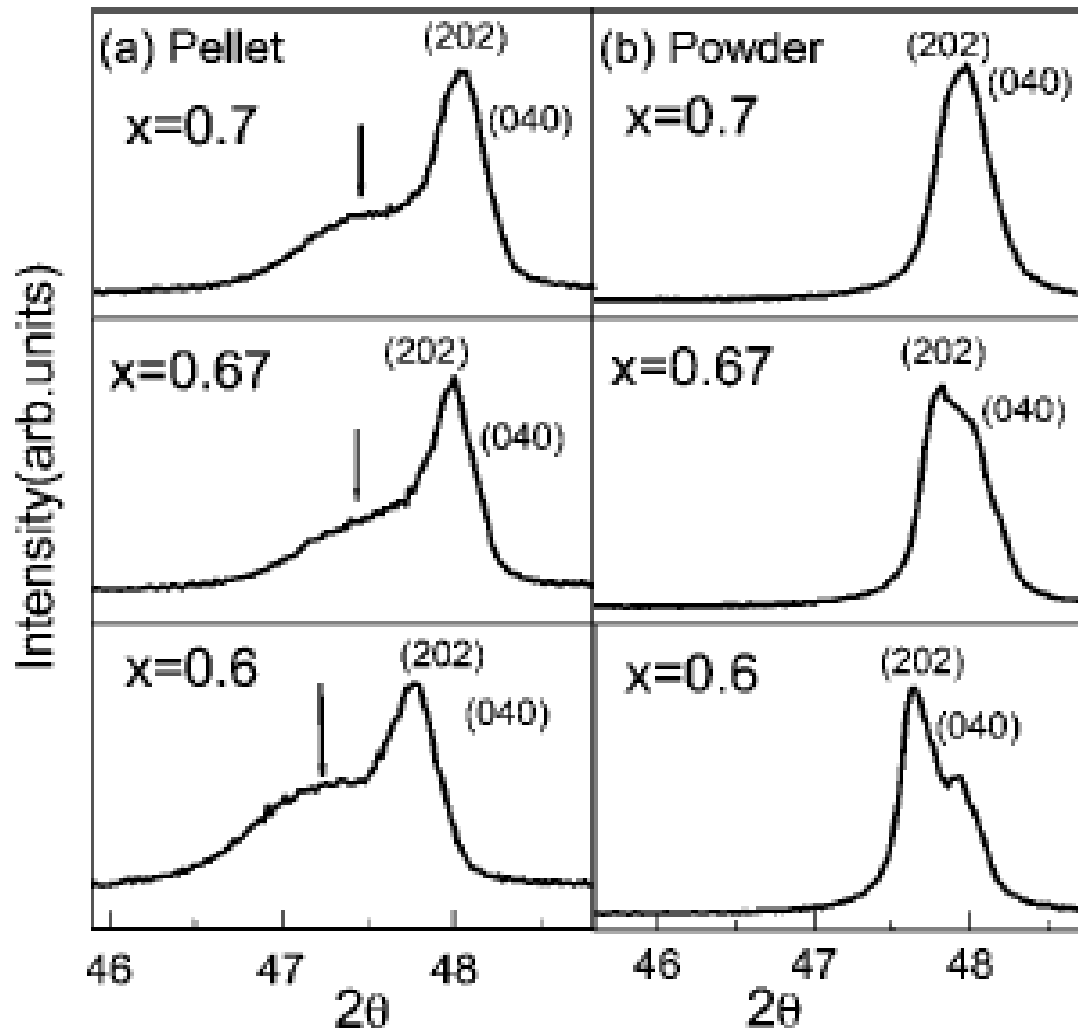
TEM Studies on LCMO $x=0.67$



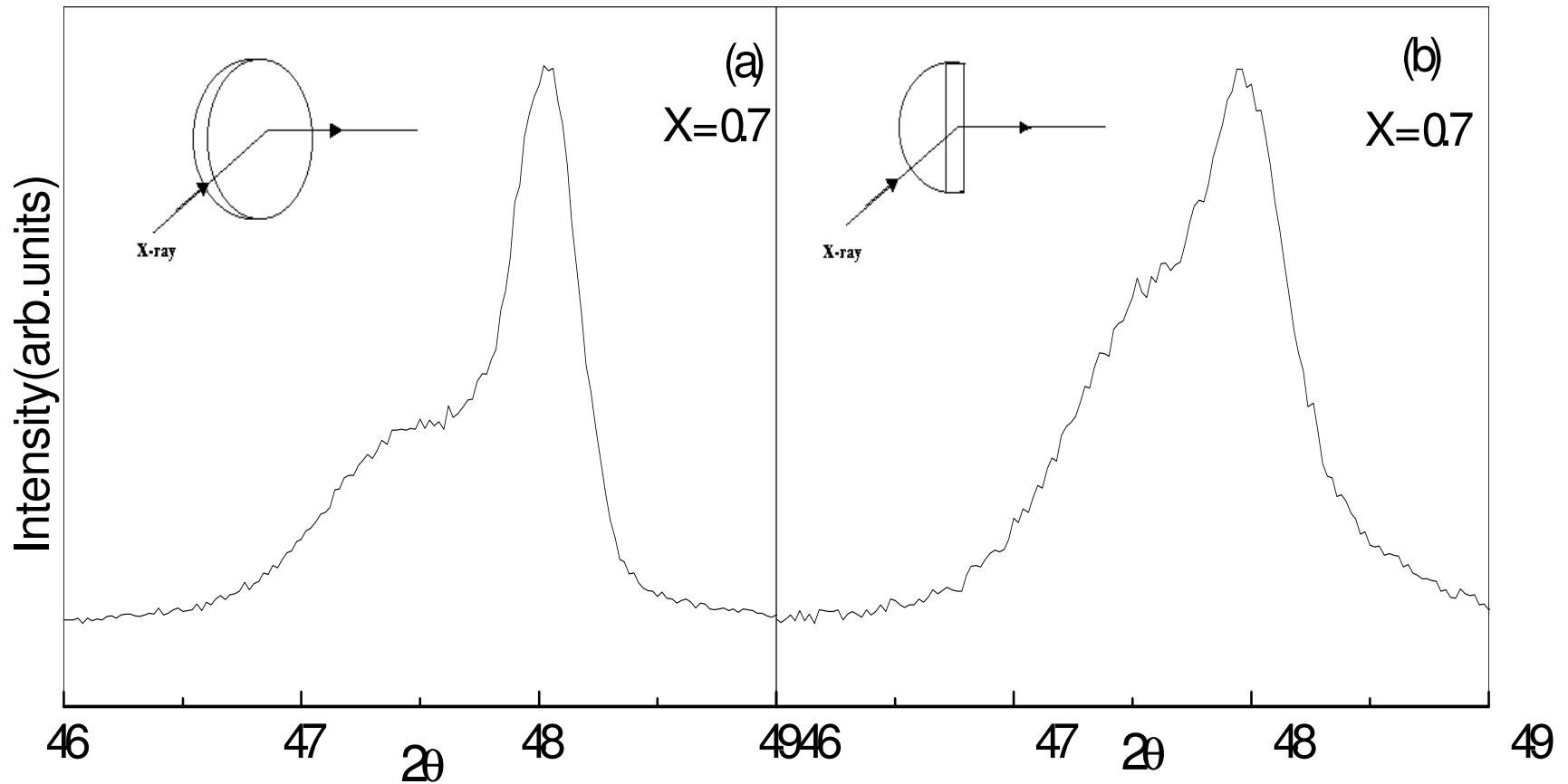
Low-temperature XRD of powdered sample of LCMO:
A negative Result



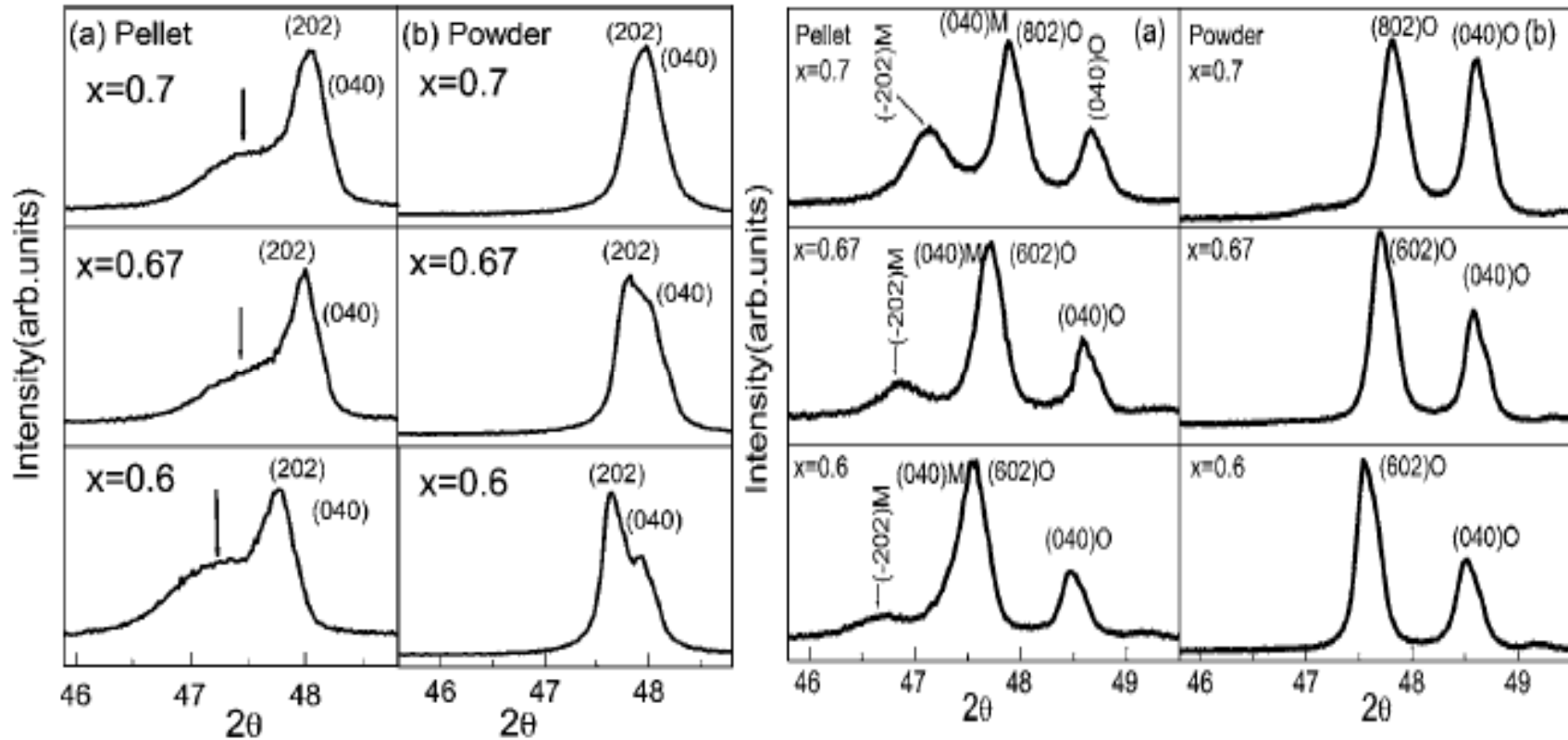
Comparison of Room Temperature XRD OF Pellet and powder for different LCMO samples



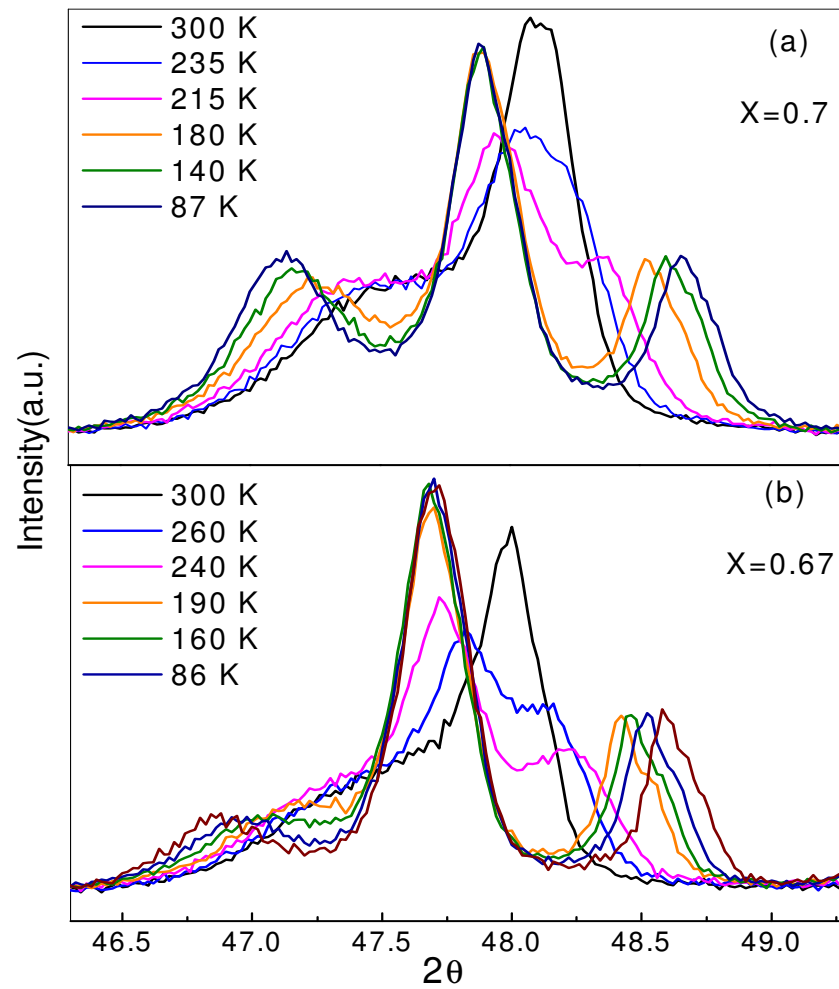
Presence of Random(Isotropic) Strained phase in a Pellet



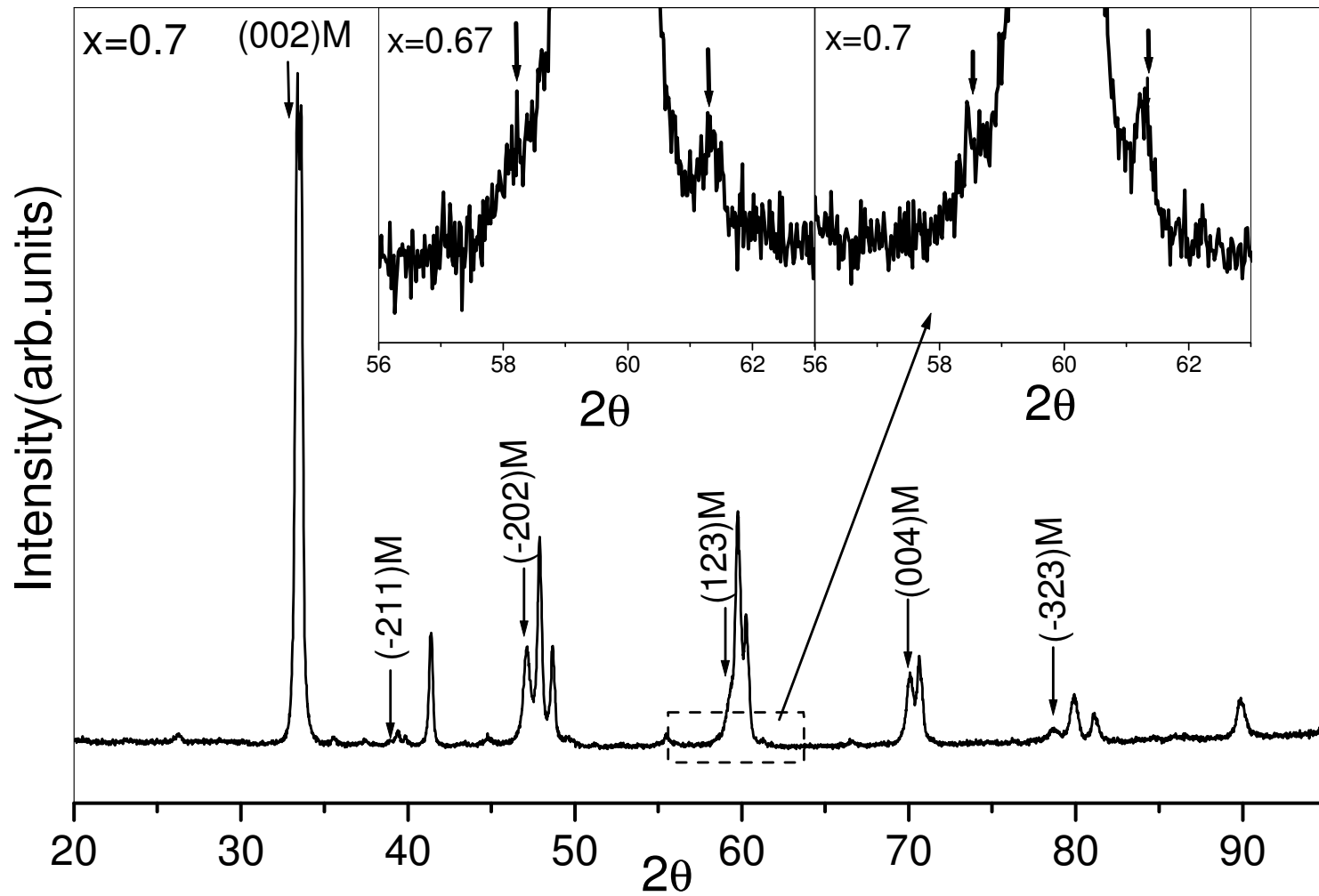
Comparison of RT and LT XRD



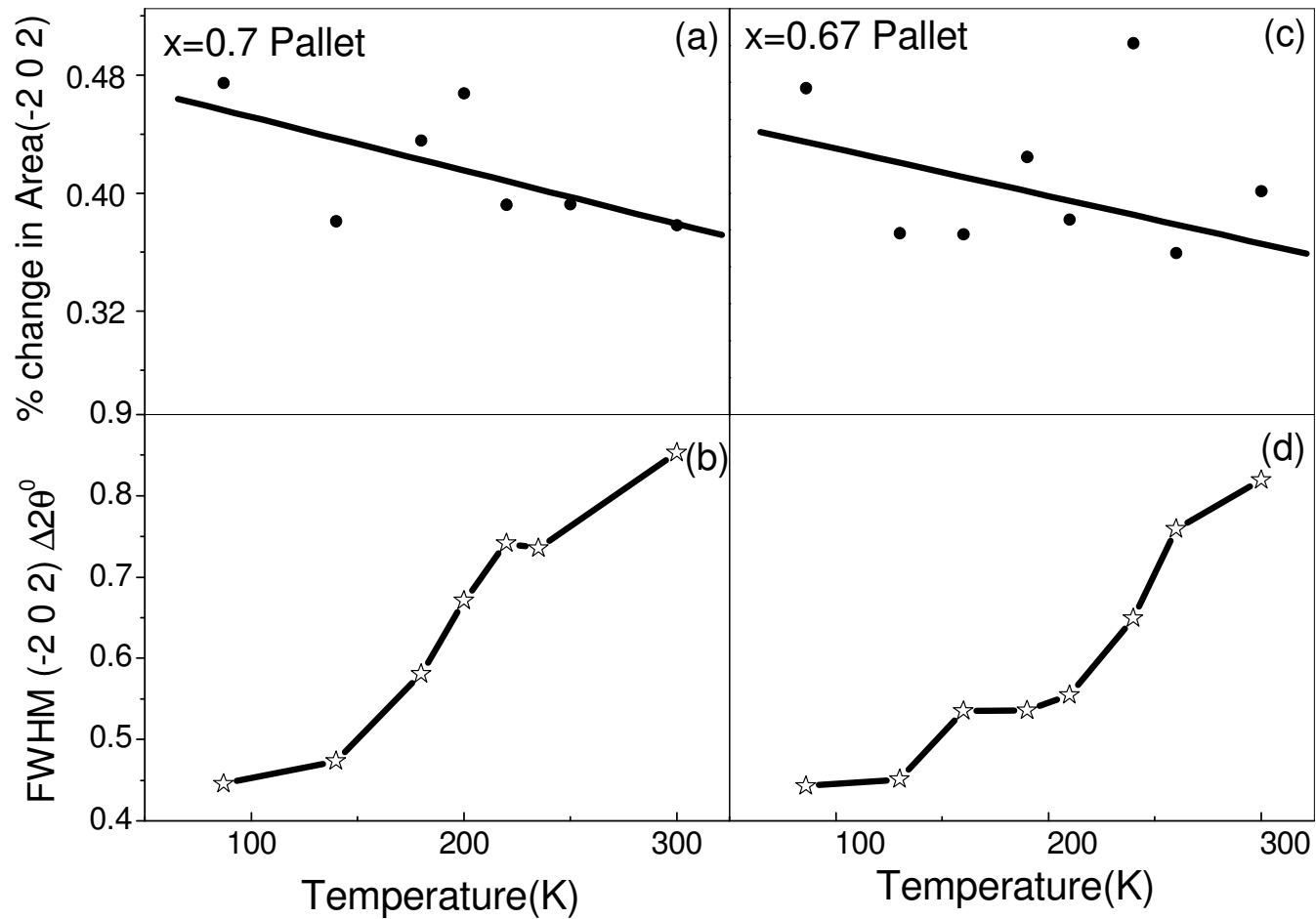
Temperature variation of XRD-Profiles



Low-temperature XRD of Pellets at 87 K

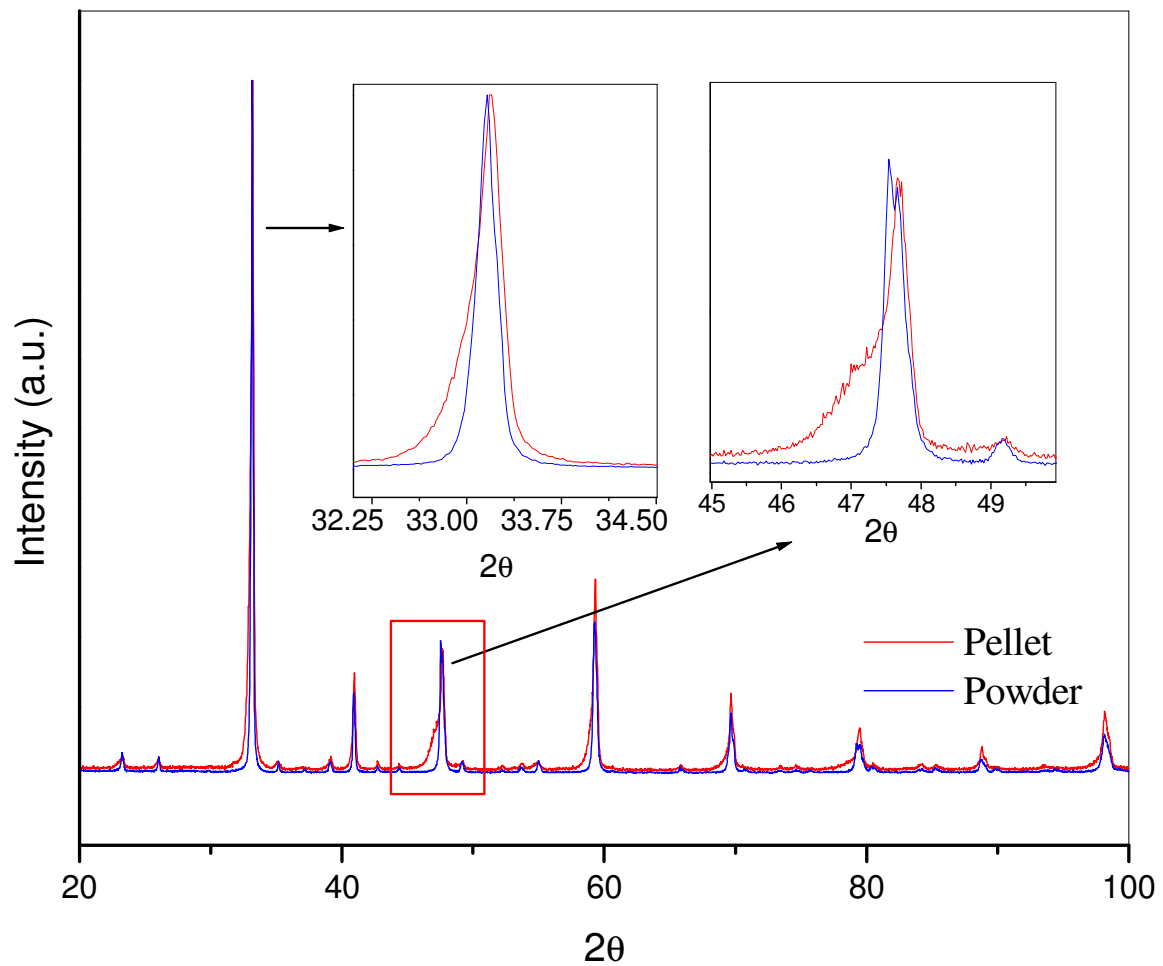


Area and FWHM of Monoclinic phase

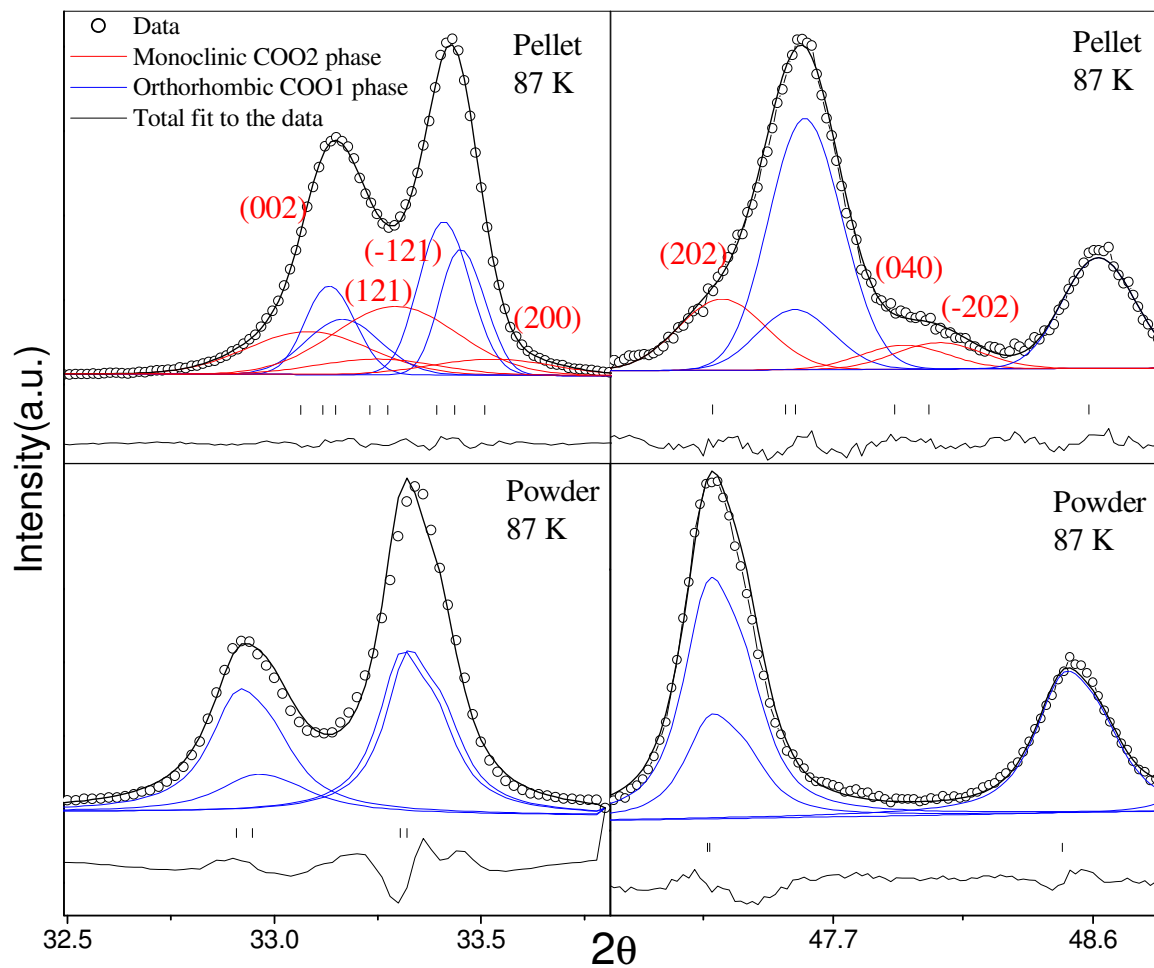


P.R.Sagdeo, S.Anwar and N.P.Lalla, Phys. Rev. B **74**, 214118 (2006)

Comparison of XRD of PCMO(5050) pellet and powder

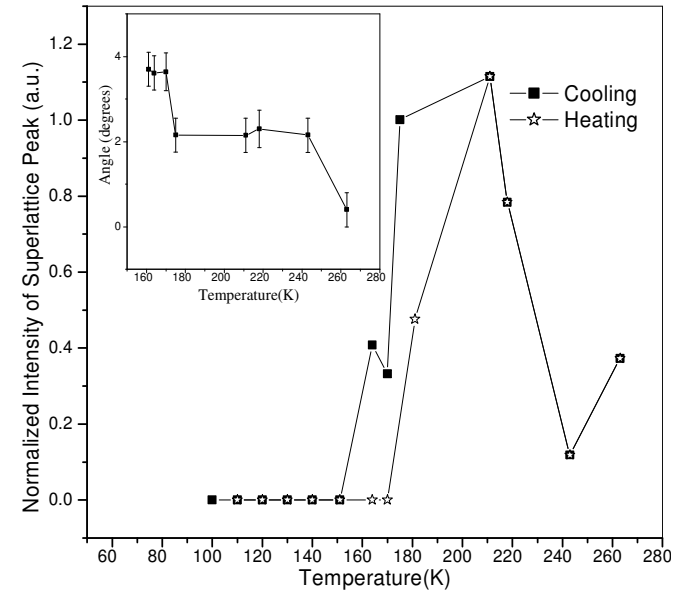
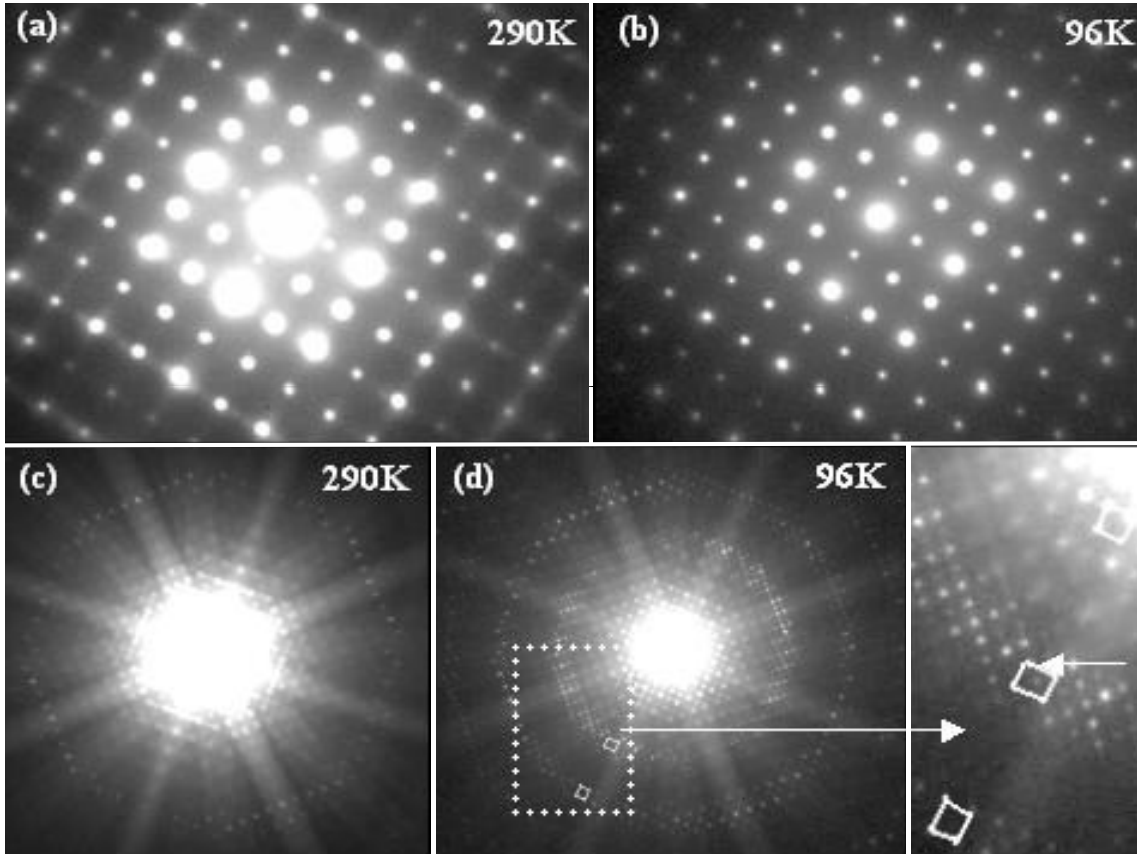


Strain induced e_g Orbital-Flipping transition

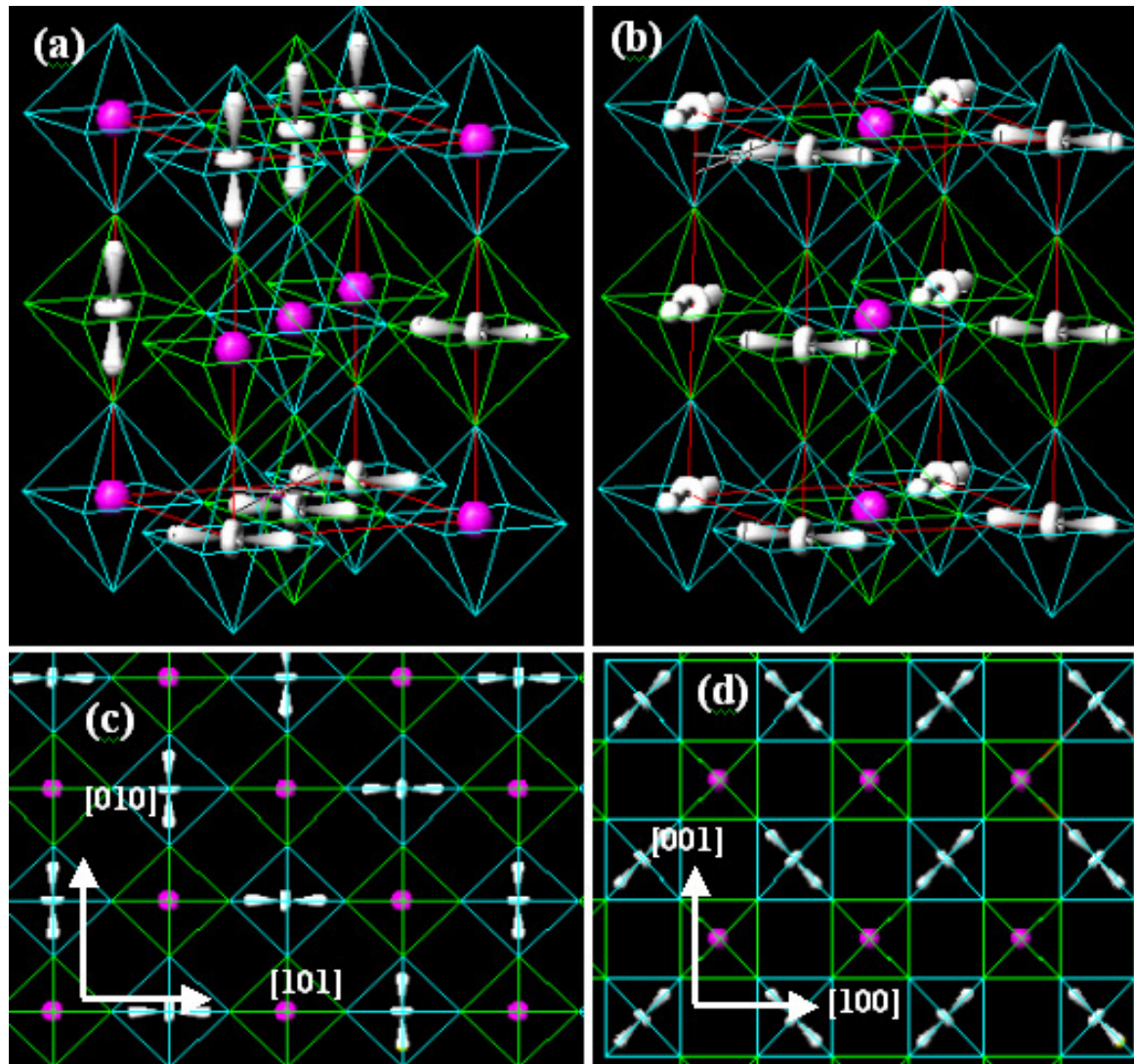


P.R.Sagdeo, N.P.Lalla, A.V.Narlikar, D.Prabhakaran, A.T.Boothroyd, Phys. Rev. B 78 174106 (2008)

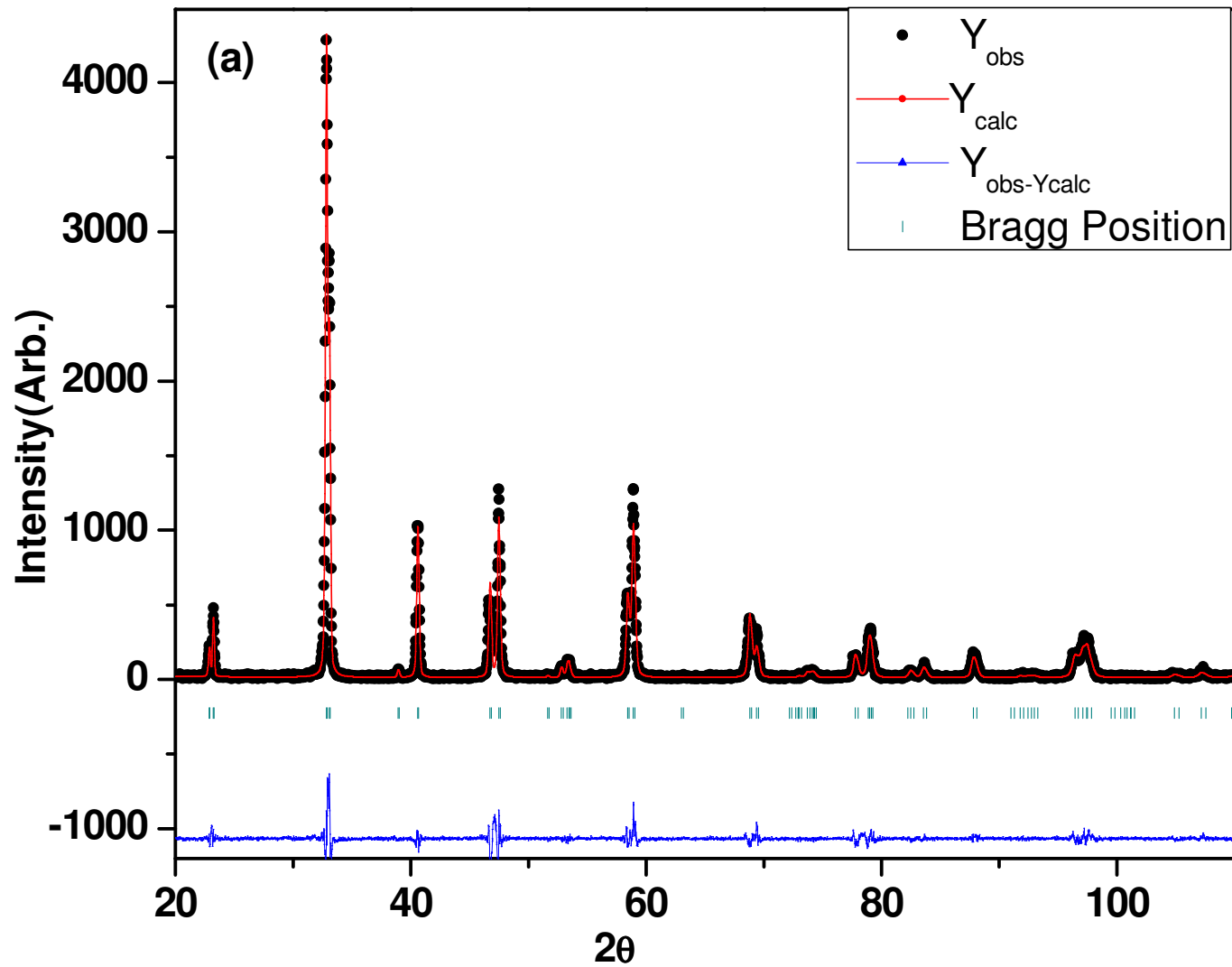
Transformation of COO1 to COO2



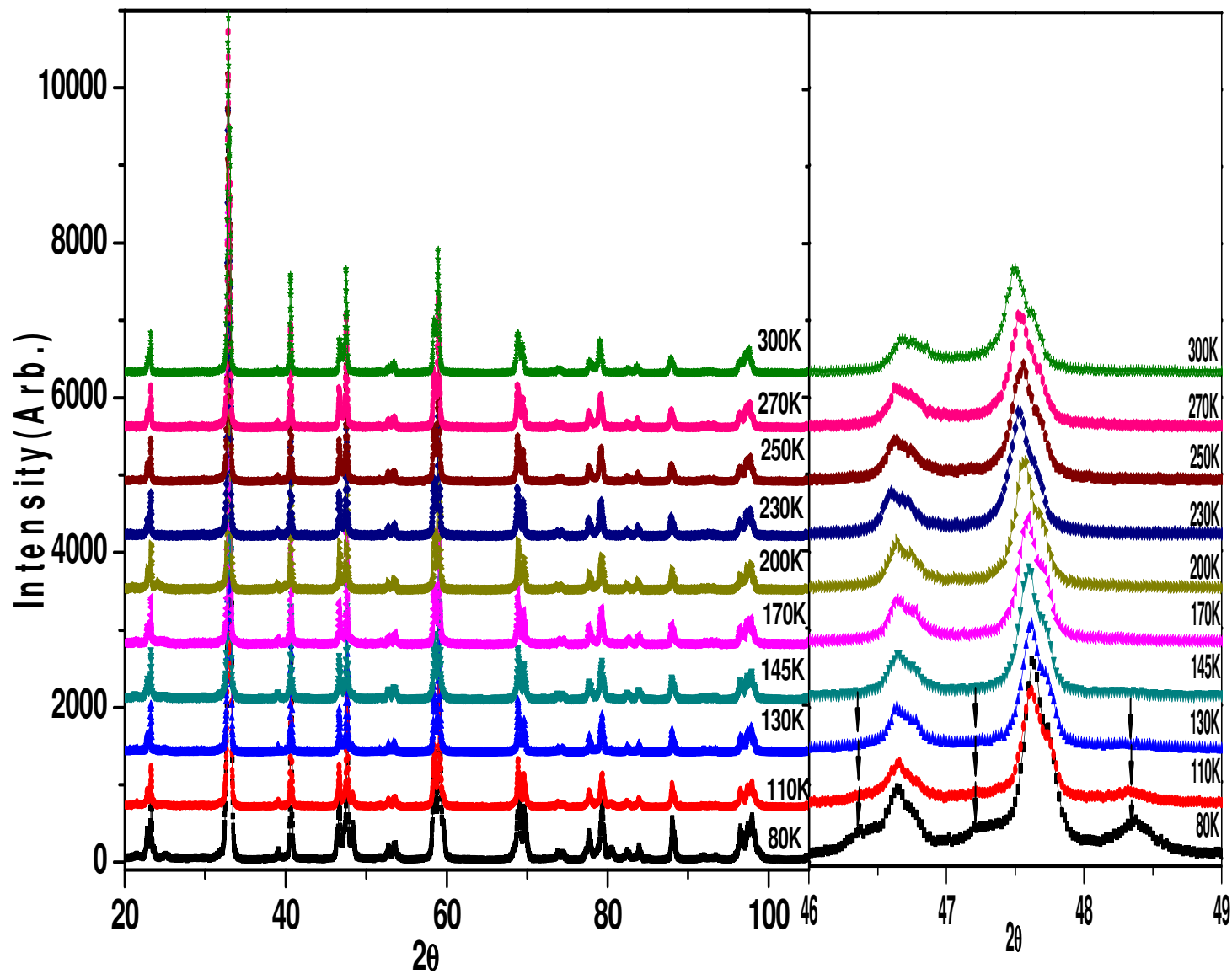
Orbital-Flipping Transition



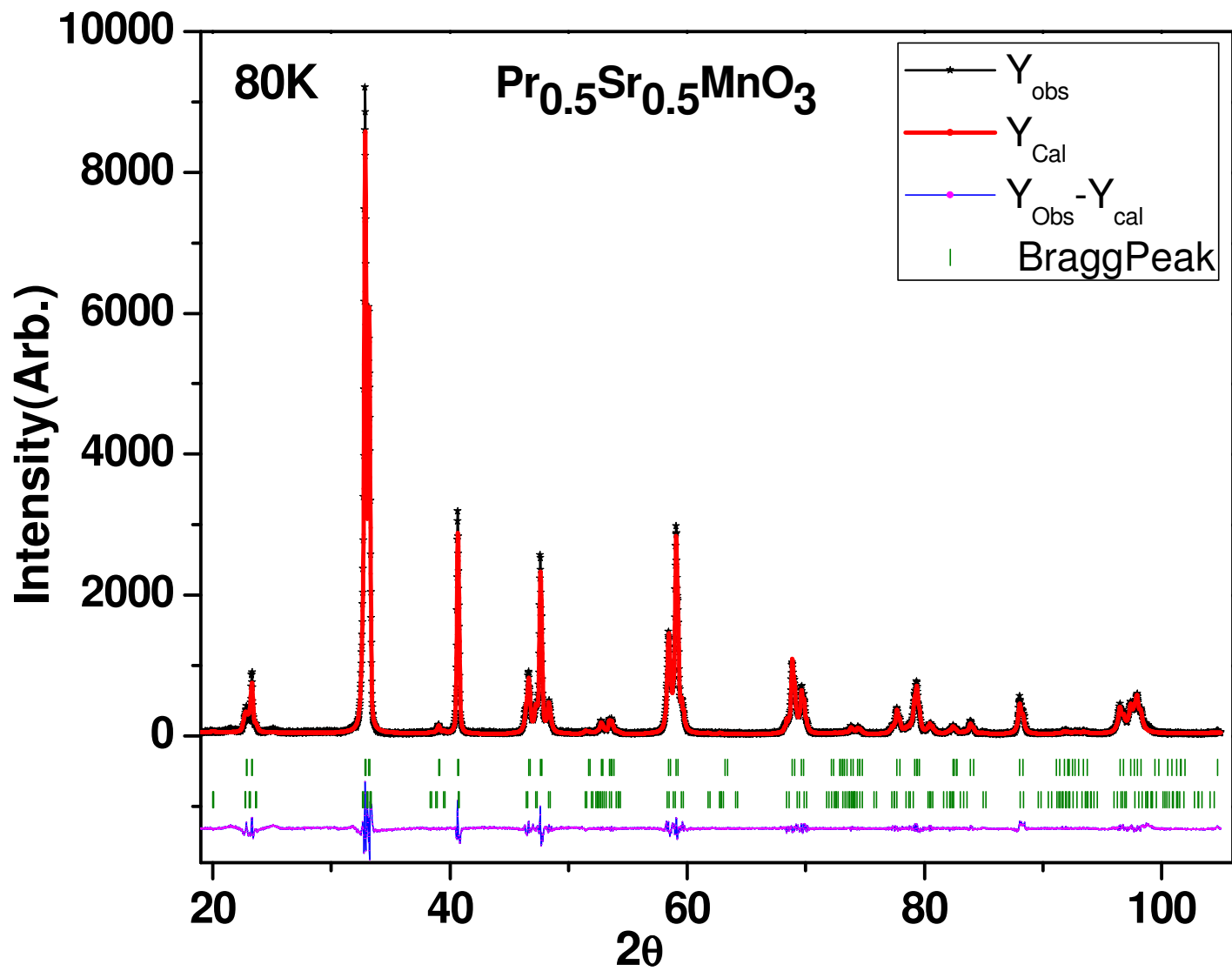
Coexistence of I4/mcm(FMM) & Fmmm(AFMI) phases in
A-Type AFM in $\text{Pr}_{0.5}\text{Sr}_{0.5}\text{MnO}_3$



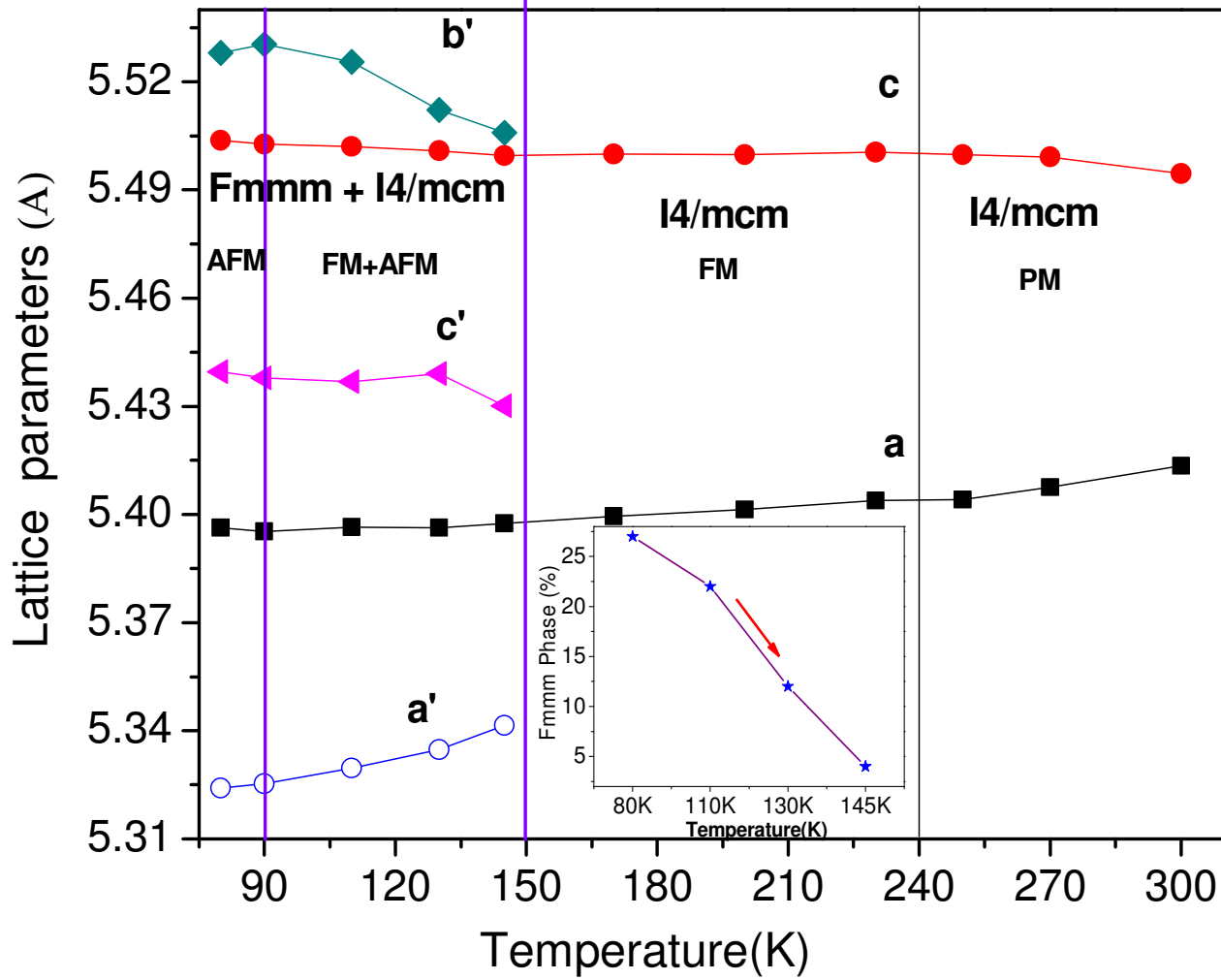
Low-Temperature Powder X-ray diffraction



Two-phase Profile Matching in $\text{Pr}_{0.5}\text{Sr}_{0.5}\text{MnO}_3$



Lattice parameter and Phase fraction variation with Temperature $\text{Pr}_{0.5}\text{Sr}_{0.5}\text{MnO}_3$



Conclusions

X-ray diffraction can be used for phase identification of the materials in a variety of forms (micro,nano etc.).

In conjunction with the Reitveld analysis it can used as a tool for accurate structural parameter determination, study of phase transformation and in some cases even for structure solution too.

Non ambient XRD can be used to study the phase transitions and phase coexistence leading to study of deep physics of Materials.